International Journal of Non–Linear Mechanics 179 (2025) 105246

Contents lists available at ScienceDirect

International Journal of Non-Linear Mechanics

journal homepage: www.elsevier.com/locate/nlm

Static bifurcations of short FPU softening chains with second-order interaction: The non-degenerate case

Angelo Luongo [a], Manuel Ferretti [a,*], Noël Challamel [b]

[a] Department of Civil, Construction-Architectural and Environmental Engineering, University of L'Aquila, 67100 L'Aquila, Italy
[b] Institut de Recherche Dupuy de Lôme UMR CNRS 6027, Centre de Recherche, Univ. Bretagne Sud, Rue de Saint Maudé, BP 92116, 56321 Lorient cedex, France

ARTICLE INFO

Keywords:
Fermi–Pasta–Ulam chain
Static bifurcation
Post-bifurcation
Buckling
Stability
Limit point

ABSTRACT

Fermi–Pasta–Ulam chains, made of $n = 2, 3, 4$ masses, taut by an end force, are considered in the static field. Each mass has a second-order interaction with the surrounding masses. Springs are of cubic type, with softening behavior. The equilibrium equations are derived by the total potential energy theorem. The fundamental nonlinear path of each chain, exhibiting a limit point, is evaluated. Then, by controlling the loading process by a displacement, instead of the force, a bifurcation analysis is carried out, to investigate both the ascending and descending branches of the fundamental path. The analysis allows evaluating the exact bifurcation points along this path, which manifest in number of $n-1$. The study also highlights the existence of a degenerate case in which all the bifurcation points coalesce at the limit point, an occurrence which is excluded here by assuming that all the bifurcation points are well-separated. The $n-1$ primary bifurcated paths are parametrically described in asymptotic form. Then, a post-bifurcation analysis is carried out along each of them, aimed at discovering further bifurcation points. Stability of all the branches found (first bifurcated and secondary bifurcated branches) is characterized from application of Lagrange–Dirichlet theorem. We show, for the present discrete nonlinear elastic systems, that for some parameters of interest, the first bifurcated branch may be stable, even if it loses stability in a secondary bifurcation scenario. The complex bifurcation scenario is depicted by 3D and 2D bifurcation diagrams, and asymptotic results validated by numerical analyses.

1. Introduction

This paper is devoted to the bifurcation analysis in nonlinear elastic lattices (*naturally discrete* periodic system) under elementary loading. Such lattices can be regarded as schematic representations of physical systems obtained by assembling elementary cells that exhibit second-order interactions and constitutive nonlinearities. Relevant applications include those discussed by Hegedüs [1] and Friedman et al. [2], who highlighted the possible occurrence of the snap-back phenomenon in self-deploying antiprismatic columns. Equally important are studies in the field of metamaterials, where several discrete systems have been employed to discuss a gallery of problems, as: devices for energy absorption and shock attenuation [3], 3D-printed soft metamaterials and cellular structures [4,5], as well as meta-biomaterials for tissue engineering [6].

The nonlinear lattice considered in this study is a one-dimensional finite lattice, with nonlinear interactions, which exhibit various well known phenomena in the field of elastic structural stability, such as limit points, bifurcation and eventually coalescence between both phenomena such as hill-top bifurcation. These phenomena are well identified and studied in structural mechanics (see for instance the seminal books of Thompson and Hunt [7]; Bažant and Cedolin [8]; Koiter [9] or Luongo et al. [10]), but the systematic investigation of bifurcation, especially secondary bifurcation phenomena, in discrete periodic system with material nonlinearities is probably less explored. The nonlinear lattice studied here is a system composed on finite number of particles connected by nonlinear restoring force of polynomial type. Such a lattice is referred to a FPU (Fermi–Pasta–Ulam) lattice, due to the first works of Fermi et al. [11] devoted to the numerical investigation of such nonlinear lattices. Fermi et al. [11] studied the vibration of such a finite lattice with three kinds of restoring forces, a cubic one, a quadratic one and a piece-wise linear one. Research on wave propagation in FPU chains have shown complex phenomena, including soliton propagation, as largely investigated by Dauxois et al. [12], Dauxois and Peyrard [13] or more recently by Vainchtein [14]. But the static response of such nonlinear lattices, even under elementary loading can also surprisingly reveal complex behaviors.

There are a significant number of papers on the static bifurcations of finite and infinite FPU systems with direct and indirect interactions, and

* Corresponding author.
E-mail addresses: angelo.luongo@univaq.it (A. Luongo), manuel.ferretti@univaq.it (M. Ferretti), noel.challamel@univ-ubs.fr (N. Challamel).

https://doi.org/10.1016/j.ijnonlinmec.2025.105246
Received 22 April 2025; Received in revised form 16 August 2025; Accepted 18 August 2025
Available online 25 August 2025
0020-7462/© 2025 The Authors. Published by Elsevier Ltd. This is an open access article under the CC BY license (http://creativecommons.org/licenses/by/4.0/).

under elementary loadings. Up to now, most of the available results are pure numerical results applied to this discrete nonlinear elastic system, with direct and indirect interactions. The seminal paper of Triantafyllidis and Bardenhagen [15] numerically explores the bifurcation of a one-dimensional nonlinear finite lattice under pure tension (including a generalized FPU system with quintic nonlinear restoring force and $p = 2$ interactions), and the capability of higher-order continuous system to capture the behaviors of the discrete system. Triantafyllidis and Bardenhagen [15] considered two types of nonlinear restoring forces, a polynomial one and a logarithmic one. The first family, the polynomial one, is a quintic restoring force which can be restricted to a cubic one, as a particular case (and then it can be classified as a generalized FPU lattice). Triantafyllidis and Bardenhagen [15] numerically detected a cascade of close bifurcation points along the fundamental path, in the vicinity of the limit point of the lattice response. A gradient elasticity continuum model has been calibrated from the nonlinear lattice and has been shown to capture the bifurcation phenomena of the lattice, for the range of parameters numerically investigated. For the parametric analysis that they conducted, i.e. for a large number of particles ($n = 96$ in the order of magnitude of hundred particles), Triantafyllidis and Bardenhagen [15] showed, in particular, that both the discrete and the strain gradient continuous approaches predict a cascade of bifurcation values, which arise just after the limit point of the bifurcation diagram. The strain gradient continuous approach predicts very close results compared to the discrete approach (numerical discrete approach). The bifurcated branches have been shown numerically to be unstable sufficiently close to the bifurcation points.

The stability of the fundamental homogeneous state in an infinite nonlinear lattice was studied later by Truskinovsky and Vainchtein [16] for nonlinear interactions based on Morse potential, and with first, second and third interactions. Combescure [17] applied the same methodology for polynomial interactions of quintic type, as initially considered by Triantafyllidis and Bardenhagen [15]. Very few analytical studies have focused on the bifurcation properties of the finite lattice, even under elementary loading. Findeisen et al. [18] numerically studied the response of a nonlinear lattice (piecewise linear or with quartic interaction) under pure tension load, with only direct interactions. Challamel et al. [19] highlighted the hill-top bifurcation phenomenon present in a FPU lattice (with only direct interaction) under pure tension load, with the existence of multiple branches at the limit point, the number depends on the number of particles. The occurrence of the snap-back branch was also mentioned and an imperfection analysis was also conducted. The hill-top bifurcation is well mentioned in the literature for other structural systems such as the paradigmatic structural system recently analyzed by Tanaka et al. [20]. The hill-top bifurcation does not arise for FPU system in presence of distributed load, where localization is enforced along the critical particle of the chain (see Hérisson et al. [21]).

For the perfect FPU system with first-order interactions, Challamel et al. [19] showed that, when the springs are all equal (i.e., no imperfections are present), the multi-degenerate hill-top bifurcation occurs, in which a large number of branched paths, (i.e., $2^n - 1$, with n the number of masses), all unstable, branch off from the non-trivial fundamental path at its limit point. Successively, in a recent paper, Challamel et al. [22], introduced second-order interactions in the chain (meaning that each particle exchanges internal forces with masses two steps away, on the left and on the right). They proved a number of interesting properties of the chain, namely: (a) the higher-order internal forces destroy the coalescence among the bifurcated paths, moving them either on the left or on the right of the limit point of the fundamental path; (b) the order of the buckling modes is the 'natural' one (i.e., the lowest mode has largest half-wavelength) when bifurcations *follow* the limit point, but it is reversed (i.e., the lowest mode has smallest half-wavelength) when bifurcations *precede* the limit point (i.e., the most interesting case); (c) for a degenerate combination of the mechanical parameters, the hill-top bifurcation exists also in the second-order FPU chain, at which all branching points, of different half-wavelengths, coalesce at the limit point. The following conclusions were obtained in [22]: (i) there is a domain in the space of structural parameters, where both the discrete and the strain gradient continuous approaches predict a cascade of bifurcation values, which arise just *after* the limit point in the bifurcation diagram; here, the gradient continuous approach predicts very close results compared to the discrete approach; (ii) however, there is also a domain of structural parameters where the bifurcations *precede* the limit point and where the continuous approach cannot precisely capture the behavior of the discrete system.

The boundary in the space of structural parameters, where the validity of the continuous approach starts to fail, coincides with the condition of the so-called hill-top bifurcation (degenerate case) highlighted by Challamel et al. [19] for $p = 1$ (just one interaction or simple FPU system). Analytical expressions for buckling loads and modes of the FPU lattice with $p = 2$ interactions were obtained in Challamel et al. [22] by solving difference equations with proper boundary conditions. The study of Challamel et al. [22], which predicts the bifurcation values (linearized problem) of the discrete FPU system for all range of structural parameters, has been supported by numerical exploration. However, a systematic bifurcation diagram for all values of n (the number of particles) and in the whole space of structural parameters was not performed, including all primary and post-bifurcation range.

In this paper, we intend to extend the analysis of Challamel et al. [22] to the nonlinear field, by investigating theoretically and numerically the post-critical behavior of second-order FPU chains. However, since the problem appears to be extremely intricate, also in the approximate context of the asymptotic theory of bifurcation, attention is limited here to lattices made of few particles (namely, $n = 2, 3, 4$). The choice is also suggested by the fact that, while for long chains, there exist an extended 'internal domain', far from boundaries, in which the field difference equation holds, when the chain, instead, is short, the boundary conditions extend their influence to a significant part of the domain, making of interest their study. It is worth stressing that, since our scope is to analyze nonlinear bifurcations occurring also on the descending branch of the fundamental path, according to the asymptotic method, the bifurcation parameter cannot be identified in the load, but in a displacement, here taken as the total elongation of the chain. Thus, the interest is focused on displacement-controlled loadings. However, the force at the end of the chain is also computed as a reactive force, possibly decreasing with the displacement. In this perspective, the case $n = 2$, already studied in Challamel et al. [22] as force-controlled, is here reconsidered. The whole study is carried out under the hypothesis that the degenerateness condition discovered in the previous paper does not occur, i.e., the bifurcation values of the controlling displacement are well-separated. The case of degeneracy or nearly-degeneracy is left for future investigation.

The paper is organized as follows. In Section 2, the equilibrium equations for the three chains under study are derived, together with the relevant fundamental paths. In Section 3, (primary) bifurcations from fundamental paths are analyzed. Bifurcation points and modes are evaluated and asymptotic expressions for branching paths are obtained. In Section 4 the possible occurrence of (secondary) post-bifurcations is investigated. Here, the analysis is limited to evaluate possible bifurcation points on the primary bifurcated paths, by renouncing to a viable (but tedious) analytical evaluation of the secondary paths. In Section 5 a stability analysis of all paths so far determined is carried out analytically, based on the Lagrange–Dirichlet theorem. In Section 6 bifurcation diagrams, in 2D and 3D, are built-up, to describe the complex bifurcation scenario suffered by the three chains. Here, comparison between asymptotic and purely numerical results is also performed. Finally, in Section 7, some conclusions are drawn and a perspective of the research is outlined. Few Appendices close the paper, in some of which details are given and one of which a discussion is presented about stability of displacement- *vs* force-controlled processes.

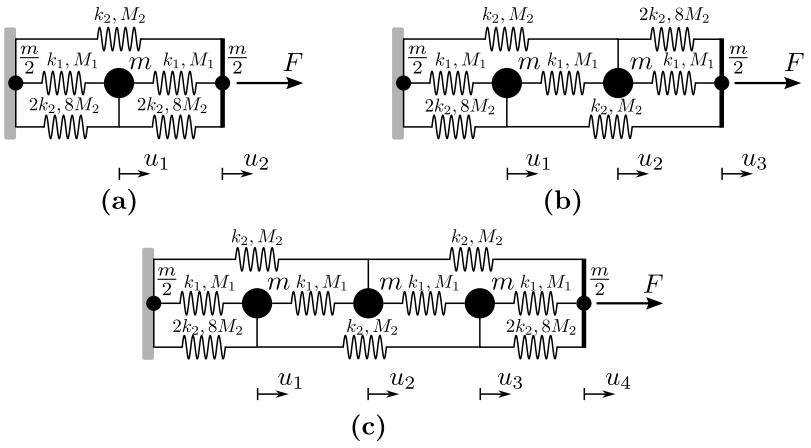

Fig. 1. Chain models: (a) two-masses, (b) three-masses, (c) four-masses.

2. Models

We consider three Fermi–Pasta–Ulam (FPU) chains with second-order interactions, made of $n = 2, 3, 4$ equispaced masses, a distance a apart (Fig. 1). The first-order interaction is exerted by springs of linear stiffness $k_1 > 0$ and cubic stiffness $M_1 > 0$, connecting adjacent masses. The second-order interaction by springs of stiffnesses $k_2 > 0$, $M_2 > 0$, connecting alternate masses. To account for boundary conditions, springs of 'half length' are considered, and therefore having stiffnesses amplified by 2 (the linear ones) or 8 (the cubic ones). The chain is fixed at the left end and free at the right end, where a force F is applied. The displacements of the masses u_i $(i = 1, 2, \dots, n)$ are taken as Lagrangian parameters. In the paper, we will mainly consider a displacement-controlled loading mode, where the end displacement is prescribed. The case of the force-controlled loading mode will be also discussed in a secondary step.

The elastic energy of a single fixed-free spring, undergoing a displacement u at its free end, is:

$$U = \frac{1}{2}k_j u^2 - \frac{1}{4a^2}M_j u^4, \qquad j = 1, 2. \tag{1}$$

The axial force in the spring, $F := \frac{\mathrm{d}U}{\mathrm{d}u}$, is:

$$F = k_j u - \frac{1}{a^2}M_j u^3. \tag{2}$$

This is a soft constitutive law, exhibiting a limit point. Referring to the spring 1, it occurs at:

$$u_l := a\sqrt{\frac{k_1}{3M_1}}, \qquad F_l := \frac{2}{3}k_1 u_l. \tag{3}$$

Equilibrium equations. We derive the equilibrium equations of the FPU chains by using the Total Potential Energy (TPE) theorem. When $n = 2$ (Fig. 1a) the TPE reads:

$$\begin{aligned} W = {} & \frac{1}{2}(k_1 + 2k_2)u_1^2 - \frac{1}{4a^2}\left(M_1 + 8M_2\right)u_1^4 + \frac{1}{2}(k_1 + 2k_2)\left(u_2 - u_1\right)^2 \\ & - \frac{1}{4a^2}\left(M_1 + 8M_2\right)\left(u_2 - u_1\right)^4 + \frac{1}{2}k_2 u_2^2 - \frac{1}{4a^2}M_2 u_2^4 - F u_2. \end{aligned} \tag{4}$$

The following nondimensional parameters and variables are introduced:

$$\alpha := \frac{k_2}{k_1}, \quad \beta := \frac{M_2}{M_1}, \quad \mu := \frac{F}{F_l}, \quad \tilde{u}_i = \frac{u_i}{u_l}, \tag{5}$$

with (u_l, F_l) defined in Eq. (3). Here, α and β are second-to-first order stiffness ratios for linear and cubic elastic forces, respectively. Accordingly, the larger α, β, the large is the weight of the higher-order internal forces in the chain. By using the definitions in Eq. (5), letting $\tilde{W} := \frac{W}{k_1 u_l^2}$ and omitting all tildes, the TPE reads:

$$\begin{aligned} W = {} & \frac{1}{2}(1 + 2\alpha)u_1^2 - \frac{1}{12}(1 + 8\beta)u_1^4 + \frac{1}{2}(1 + 2\alpha)\left(u_2 - u_1\right)^2 \\ & - \frac{1}{12}(1 + 8\beta)\left(u_2 - u_1\right)^4 + \frac{1}{2}\alpha u_2^2 - \frac{1}{12}\beta u_2^4 - \frac{2}{3}\mu u_2. \end{aligned} \tag{6}$$

The equilibrium equations are drawn from the stationary conditions $\frac{\partial W}{\partial u_i} = 0$, $i = 1, 2$, which provides:

$$\begin{bmatrix} 2 + 4\alpha & -(1 + 2\alpha) \\ -(1 + 2\alpha) & 1 + 3\alpha \end{bmatrix}\begin{pmatrix} u_1 \\ u_2 \end{pmatrix} + \begin{pmatrix} f_1\left(u_1, u_2\right) \\ f_2\left(u_1, u_2\right) \end{pmatrix} = \mu\begin{pmatrix} 0 \\ \frac{2}{3} \end{pmatrix}, \tag{7}$$

where:

$$\begin{pmatrix} f_1 \\ f_2 \end{pmatrix} := \frac{1}{3}\begin{pmatrix} (1 + 8\beta)\left[\left(u_2 - u_1\right)^3 - u_1^3\right] \\ (1 + 8\beta)\left(u_1 - u_2\right)^3 - \beta u_2^3 \end{pmatrix}. \tag{8}$$

By proceeding in the same way, the following nondimensional equilibrium equations are drawn for $n = 3$ (Fig. 1b):

$$\begin{bmatrix} 2 + 3\alpha & -1 & -\alpha \\ -1 & 2 + 3\alpha & -1 - 2\alpha \\ -\alpha & -1 - 2\alpha & 1 + 3\alpha \end{bmatrix}\begin{pmatrix} u_1 \\ u_2 \\ u_3 \end{pmatrix} + \begin{pmatrix} f_1\left(u_i\right) \\ f_2\left(u_i\right) \\ f_3\left(u_i\right) \end{pmatrix} = \mu\begin{pmatrix} 0 \\ 0 \\ \frac{2}{3} \end{pmatrix}, \tag{9}$$

and for $n = 4$ (Fig. 1c):

$$\begin{bmatrix} 2 + 3\alpha & -1 & -\alpha & 0 \\ -1 & 2 + 2\alpha & -1 & -\alpha \\ -\alpha & -1 & 2 + 3\alpha & -1 - 2\alpha \\ 0 & -\alpha & -1 - 2\alpha & 1 + 3\alpha \end{bmatrix}\begin{pmatrix} u_1 \\ u_2 \\ u_3 \\ u_4 \end{pmatrix} + \begin{pmatrix} f_1\left(u_i\right) \\ f_2\left(u_i\right) \\ f_3\left(u_i\right) \\ f_4\left(u_i\right) \end{pmatrix} = \mu\begin{pmatrix} 0 \\ 0 \\ 0 \\ \frac{2}{3} \end{pmatrix}, \tag{10}$$

where $f_j\left(u_i\right)$ are cubic homogeneous functions. Details are reported in Appendix A.

Fundamental path. The equilibrium Eqs. (7), (9) and (10) admit the following solutions, describing the *non-trivial fundamental path* $\mathcal{F}$:

$$\hat{u}_1 = \frac{1}{n}\Delta, \ \dots, \ \hat{u}_i = \frac{i}{n}\Delta, \ \dots, \ \hat{u}_{n-1} = \frac{n-1}{n}\Delta, \quad n = 2, 3, 4, \tag{11}$$

where $\Delta := u_n$ is the total elongation, satisfying the last of the equilibrium equation, namely:

$$n = 2: \quad \hat{\mu} = \frac{1}{4}\Delta\left[3(1 + 4\alpha) - \frac{1}{4}(1 + 16\beta)\Delta^2\right], \tag{12a}$$

$$n = 3: \quad \hat{\mu} = \frac{1}{2}\Delta\left[(1 + 4\alpha) - \frac{1}{27}(1 + 16\beta)\Delta^2\right], \tag{12b}$$

$$n = 4: \quad \hat{\mu} = \frac{1}{8}\Delta\left[3(1 + 4\alpha) - \frac{1}{16}(1 + 16\beta)\Delta^2\right]. \tag{12c}$$

It is easy to check that a limit point L occurs, in the three cases, at:

$$\Delta_L := n\sqrt{\frac{1 + 4\alpha}{1 + 16\beta}}, \quad \mu_L := \sqrt{\frac{(1 + 4\alpha)^3}{1 + 16\beta}}, \qquad n = 2, 3, 4, \tag{13}$$

i.e., at the same value of the force μ_L, and at the same value of the specific elongation $\frac{\Delta_L}{n}$.

Displacement-controlled loadings. In what follows, it is found more convenient, to consider loading processes governed by the end displacement $\Delta := u_n > 0$,[1] instead of the load. This procedure is suggested by the occurrence of the limit point L on the fundamental path, which makes no possibility of taking the load as bifurcation parameter, if also the softening behavior is of interest. Moreover, the approach permits to reduce to $n-1$ the degrees of freedom of the system, namely $\mathbf{u} := (u_1, \dots, u_{n-1})$, so that the Lagrangian equilibrium equations are the first $n-1$ of Eqs. (7), (9) or (10). Once displacements have been computed, the last scalar equation provides the reactive force μ.

The equilibrium equations for the three chains, accordingly, transform as follows:

$$n=2: \ (2+4\alpha)\,u_1 + f_1(u_1;\Delta) = \Delta(1+2\alpha), \tag{14a}$$

$$n=3: \ \begin{bmatrix} 2+3\alpha & -1 \\ -1 & 2+3\alpha \end{bmatrix} \begin{pmatrix} u_1 \\ u_2 \end{pmatrix} + \begin{pmatrix} f_1(u_i;\Delta) \\ f_2(u_i;\Delta) \end{pmatrix} = \Delta \begin{pmatrix} \alpha \\ 1+2\alpha \end{pmatrix}, \tag{14b}$$

$$n=4: \ \begin{bmatrix} 2+3\alpha & -1 & -\alpha \\ -1 & 2+2\alpha & -1 \\ -\alpha & -1 & 2+3\alpha \end{bmatrix} \begin{pmatrix} u_1 \\ u_2 \\ u_3 \end{pmatrix} + \begin{pmatrix} f_1(u_i;\Delta) \\ f_2(u_i;\Delta) \\ f_3(u_i;\Delta) \end{pmatrix} = \Delta \begin{pmatrix} 0 \\ \alpha \\ 2\alpha \end{pmatrix}. \tag{14c}$$

In this perspective, the TPE (needed to detect stability) is still given by Eq. (6) and analogous in Appendix B, but deprived of the load term, which expresses a reactive work. For later purposes, the Hessian matrices of the TPE, i.e., $\mathbf{K}(\mathbf{u};\Delta) := \left[\frac{\partial^2 W}{\partial u_i \partial u_j}\right]$,[2] are computed in Appendix A.

3. Primary bifurcations

An asymptotic bifurcation analysis is carried out to detect bifurcation points C_m and relevant *primary bifurcated paths* $\mathcal{P}_m$ branching from the fundamental path $\mathcal{F}$.

3.1. Perturbation equations

We consider the equilibrium Eq. (14), in which we express the unknowns u_i in the following incremental form:

$$u_i = \hat{u}_i + v_i, \qquad i = 1, \dots, n-1 \quad . \tag{15}$$

Moreover, we describe the bifurcated paths by parametric equations $v_i = v_i(\epsilon)$, $\Delta = \Delta(\epsilon)$, where ϵ is a parameter, taken zero at the bifurcation point. By expanding the parametric equations, starting from $\epsilon = 0$, we have:

$$v_i(\epsilon) = \epsilon \dot{v}_{ic} + \epsilon^2 \ddot{v}_{ic} + \epsilon^3 \dddot{v}_{ic}, \tag{16a}$$

$$\Delta(\epsilon) = \Delta_c + \epsilon \dot{\Delta}_c + \epsilon^2 \ddot{\Delta}_c. \tag{16b}$$

Here and ahead, we use the notation $\dot{q}_c := \frac{\mathrm{d}q}{\mathrm{d}\epsilon}\Big|_{\epsilon=0}$, $\ddot{q}_c := \frac{1}{2}\frac{\mathrm{d}^2 q}{\mathrm{d}\epsilon^2}\Big|_{\epsilon=0}$, $\dddot{q}_c := \frac{1}{6}\frac{\mathrm{d}^3 q}{\mathrm{d}\epsilon^3}\Big|_{\epsilon=0}$, for any magnitude $q = q(\epsilon)$ on the path.

By separately equating to zero the terms with the same powers of ϵ in Eq. (14), we get perturbation equations of the form:

$$\epsilon^1: \quad \mathbf{K}_c \dot{\mathbf{v}}_c = \mathbf{0}, \tag{17a}$$

$$\epsilon^2: \quad \mathbf{K}_c \ddot{\mathbf{v}}_c = -\ddot{\mathbf{f}}_c(\dot{\mathbf{v}}, \dot{\Delta}_c), \tag{17b}$$

$$\epsilon^3: \quad \mathbf{K}_c \dddot{\mathbf{v}}_c = -\dddot{\mathbf{f}}_c(\dot{\mathbf{v}}_c, \ddot{\mathbf{v}}_c, \dot{\Delta}_c, \ddot{\Delta}_c). \tag{17c}$$

Here, $\mathbf{K}_c := \mathbf{K}(\hat{\mathbf{u}}(\Delta_c);\Delta_c)$ (see Appendix A) is the tangent stiffness matrix at the (unknown) branching point; $\mathbf{v} := (v_1, \dots, v_{n-1})^T$ is the unknown vector, and $\ddot{\mathbf{f}}_c$, $\dddot{\mathbf{f}}_c$ are 'known term vectors', since they depend on quantities evaluated at the previous steps. Eq. (17a) is first solved for the three chains (Section 3.2), in order to find one or more bifurcation points C_m on $\mathcal{F}$; then (Section 3.3), Eqs. (17b), (17c) are tackled to build-up the bifurcated paths $\mathcal{P}_m$ emanating from $\mathcal{F}$ at C_m.

3.2. Bifurcation points and critical modes

The first of the perturbation Eq. (17) is solved for the three chains, to find the critical values Δ_{cm} ($m = 1, 2, \dots$) of the bifurcation parameter Δ and the associated critical modes $\dot{\mathbf{v}}_{cm}$ (here normalized as $\max|\dot{\mathbf{v}}_{cm}| = 1$).

Two-mass chain. When $n = 2$, Eq. (17a) reads:

$$\left[2 + 4\alpha - \frac{1}{2}(1+8\beta)\Delta_c^2\right]\dot{v}_1 = 0, \tag{18}$$

so that just *one* primary bifurcation point C_1 exists, at which:

$$C_1: \qquad \Delta_{c1} := 2\sqrt{\frac{1+2\alpha}{1+8\beta}}, \qquad \dot{\mathbf{v}}_{c1} := (1)^T. \tag{19}$$

By recalling that the limit point of the fundamental path occurs at Δ_L, as given by the first of Eq. (13), we observe that:

- when $\alpha < 4\beta$, then $\Delta_L < \Delta_{c1}$, i.e., the bifurcation points *follows* the limit point;
- when $\alpha > 4\beta$, then $\Delta_{c1} < \Delta_L$, i.e., the bifurcation point *precedes* the limit point;
- when $\alpha = 4\beta$, then $\Delta_L = \Delta_{c1}$, i.e., the bifurcation point coalesces with the limit point.

Three-mass chain. When $n = 3$, Eq. (17a) reads:

$$\begin{bmatrix} 2+3\alpha - \frac{1}{3}\left(\frac{2}{3}+4\beta\right)\Delta_c^2 & -1 + \frac{\Delta_c^2}{9} \\ \text{SYM} & 2+3\alpha - \frac{1}{3}\left(\frac{2}{3}+4\beta\right)\Delta_c^2 \end{bmatrix} \begin{pmatrix} \dot{v}_1 \\ \dot{v}_2 \end{pmatrix} = \begin{pmatrix} 0 \\ 0 \end{pmatrix}. \tag{20}$$

Since the characteristic equation is quadratic in Δ_c^2, *two* primary bifurcation points $C_{1,2}$ are found, at which:

$$C_1: \quad \Delta_{c1} := 3\sqrt{\frac{1+3\alpha}{1+12\beta}}, \qquad \dot{\mathbf{v}}_{c1} := (1,1)^T, \tag{21a}$$

$$C_2: \quad \Delta_{c2} := 3\sqrt{\frac{1+\alpha}{1+4\beta}}, \qquad \dot{\mathbf{v}}_{c2} := (1,-1)^T. \tag{21b}$$

By recalling the definition of the limit point in Eq. (13), we observe that:

- when $\alpha < 4\beta$, then $\Delta_L < \Delta_{c1} < \Delta_{c2}$, i.e., the two bifurcation points *follow* the limit point;
- when $\alpha > 4\beta$, then $\Delta_{c2} < \Delta_{c1} < \Delta_L$, i.e., the two bifurcation points *precede* the limit point;
- when $\alpha = 4\beta$, then $\Delta_L = \Delta_{c1} = \Delta_{c2}$, i.e., the two bifurcation points coalesce at the limit point.

It appears that, when $\alpha < 4\beta$, the chain buckles in a mode, $\dot{\mathbf{v}}_{c1}$, in which the displacements have the same sign; when, instead, $\alpha > 4\beta$, the chain buckles in a mode, $\dot{\mathbf{v}}_{c2}$, in which the displacements have opposite sign. The buckling modes, according to [22], are sampled sinusoidal functions, namely: of half-wavelength L in mode 1 and of half-wavelength $L/2$ in mode 2, with $L = 3a$ the total length of the chain.

Four-mass chain. When $n = 4$, Eq. (17a) reads:

$$\begin{bmatrix} 2+3\alpha & -1+\frac{\Delta_c^2}{16} & -\alpha+\frac{1}{4}\beta\Delta_c^2 \\ -\frac{1}{8}(1+6\beta)\Delta_c^2 & & \\ & 2+2\alpha & -1+\frac{\Delta_c^2}{16} \\ & -\frac{1}{8}(1+4\beta)\Delta_c^2 & \\ & & 2+3\alpha \\ \text{SYM} & & -\frac{1}{8}(1+6\beta)\Delta_c^2 \end{bmatrix} \begin{pmatrix} \dot{v}_1 \\ \dot{v}_2 \\ \dot{v}_3 \end{pmatrix} = \begin{pmatrix} 0 \\ 0 \\ 0 \end{pmatrix}. \tag{22}$$

[1] Indeed, $\Delta < 0$ provides symmetric solutions, for which $\mu < 0$.

[2] Although the work of the force should be suppressed in this expression, it is inessential in establishing the second derivatives of W.

Since the characteristic equation is cubic in Δ_c^2, *three* primary bifurcation points $C_{1,2,3}$ are found, i.e.[3]:

$$C_1:\ \Delta_{c1}:=4\sqrt{\frac{1+2\alpha+\sqrt{2}(\alpha-4\beta)+8\beta(1+\alpha)}{1+16\beta+32\beta^2}},\ \dot{\mathbf{v}}_{c1}:=\left(\frac{\sqrt{2}}{2},1,\frac{\sqrt{2}}{2}\right)^T, \tag{24a}$$

$$C_2:\ \Delta_{c2}:=4\sqrt{\frac{1+2\alpha}{1+8\beta}},\ \dot{\mathbf{v}}_{c2}:=(1,0,-1)^T, \tag{24b}$$

$$C_3:\ \Delta_{c3}:=4\sqrt{\frac{1+2\alpha-\sqrt{2}(\alpha-4\beta)+8\beta(1+\alpha)}{1+16\beta+32\beta^2}},\ \dot{\mathbf{v}}_{c3}:=\left(\frac{\sqrt{2}}{2},-1,\frac{\sqrt{2}}{2}\right)^T. \tag{24c}$$

Since the limit point of the fundamental path occurs at Δ_L, as given by the first of Eq. (13), it follows, that:

- when $\alpha<4\beta$, then $\Delta_L<\Delta_{c1}<\Delta_{c2}<\Delta_{c3}$, i.e., the three bifurcation points *follow* the limit point;
- when $\alpha>4\beta$, then $\Delta_{c_3}<\Delta_{c_2}<\Delta_{c_1}<\Delta_L$, i.e., the three bifurcation points *precede* the limit point;
- when $\alpha=4\beta$, then $\Delta_L=\Delta_{c_1}=\Delta_{c_2}=\Delta_{c_3}$, i.e., the three bifurcation points coalesce at the limit point.

Again, when $\alpha<4\beta$, the critical mode $\dot{\mathbf{v}}_1$ has equal signs, when $\alpha>4\beta$, the critical mode $\dot{\mathbf{v}}_{c3}$ has alternate signs. The buckling modes are sampled sinusoidal functions of different half-wavelength, namely: L in mode 1, $L/2$ in mode 2 and $L/3$ in mode 3, with $L=4a$ the total length of the chain [22].

The present analysis confirms the existence of a *degenerate case*, $\alpha=4\beta$, discovered in [22], at which interaction between different bifurcations occur. As it is well-known in bifurcation analysis, the study of degenerate cases is mandatory (e.g., an iconic example of nonlinear interaction is represented by the Augusti model [10,23]), since the geometric structure of the degenerate bifurcation permits to explain (via continuous perturbations) the geometric structure of the non-degenerate cases, even when these latter are far from the coalescence. This problem will be tackled in a forthcoming paper.

3.3. Bifurcated paths

From each bifurcation point C_m a primary bifurcated path $\mathcal{P}_m$ originates from $\mathcal{F}$, that we want to express in asymptotic form (see Fig. 2 for a qualitative sketch). In this paper, we will assume that the bifurcation points C_m are all *distinct and well-separated*, i.e., $\alpha-4\beta=O(1)$. To evaluate the tangents to $\mathcal{P}_m$ at the branching points, the ϵ^2 order within Eq. (17) must be tackled. Since the stiffness matrix $\mathbf{K}_c$ is singular, the compatibility conditions $\dot{\mathbf{v}}_{cm}^T\ddot{\mathbf{f}}_c\left(\dot{\mathbf{v}}_{cm};\dot{\Delta}_{cm}\right)=0$ must hold, separately for each of the bifurcation modes; from them, $\dot{\Delta}_{cm}$ is derived. By truncating the analysis at this order, the bifurcated path is approximated by its straight tangent line at C_m. To obtain a more accurate representation, the ϵ^2 order equations must be solved for $\ddot{\mathbf{v}}_{cm}$ (e.g., by ignoring the complementary solution) and compatibility enforced at the ϵ^3 order, by requiring that $\dot{\mathbf{v}}_{cm}^T\dddot{\mathbf{f}}_c\left(\dot{\mathbf{v}}_{cm},\ddot{\mathbf{v}}_{cm};\dot{\Delta}_{cm},\ddot{\Delta}_{cm}\right)=0$ for each m; from these latter, $\ddot{\Delta}_{cm}$ is evaluated. By truncating the analysis at this order, also the curvature at C_m is captured, and the bifurcated path extrapolated as a degree-2 algebraic curve. Calculations are detailed below for the three chains.

[3] Alternative expressions for $\Delta_{c1,3}$ are:

$$\Delta_{c1,3}=4\sqrt{\frac{1+\left(2\pm\sqrt{2}\right)\alpha}{1+\left(2\pm\sqrt{2}\right)4\beta}}, \tag{23}$$

which coincide with those found in [22], namely $\left(\frac{\Delta_{cm}}{\Delta_L}\right)^2=\frac{1-\frac{4\alpha}{1+4\alpha}\sin^2\left(\frac{m\pi}{8}\right)}{1-\frac{16\beta}{1+16\beta}\sin^2\left(\frac{m\pi}{8}\right)}$, accounting for $\sin^2\left(\frac{\pi}{8}\right)=\frac{2-\sqrt{2}}{4}$, $\sin^2\left(\frac{3\pi}{8}\right)=\frac{2+\sqrt{2}}{4}$.

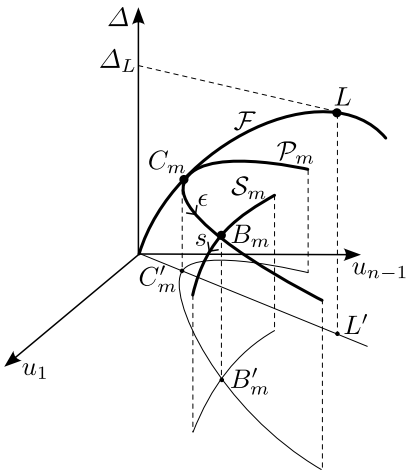

Fig. 2. Qualitative sketch of: the fundamental path $\mathcal{F}$ and its limit point L; a primary bifurcated path $\mathcal{P}_m$ emanating from C_m; a secondary bifurcated path $\mathcal{S}_m$ emanating from B_m. Points C_m and B_m can be either pitchfork or transcritical bifurcation points.

Two-mass chain. The perturbation Eq. (17) read:

$$\epsilon^1:\quad\left[2+4\alpha-\frac{1}{2}(1+8\beta)\Delta_{c1}^2\right]\dot{v}_{1c}=0, \tag{25a}$$

$$\epsilon^2:\quad\left[2+4\alpha-\frac{1}{2}(1+8\beta)\Delta_{c1}^2\right]\ddot{v}_{1c}=(1+8\beta)\Delta_{c1}\dot{\Delta}_{c1}\dot{v}_{1c}, \tag{25b}$$

$$\epsilon^3:\quad\left[2+4\alpha-\frac{1}{2}(1+8\beta)\Delta_{c1}^2\right]\dddot{v}_{1c}=(1+8\beta)\left[\Delta_{c1}\dot{\Delta}_{c1}\ddot{v}_{1c}+\frac{2}{3}\dot{v}_{1c}^3+\frac{1}{2}\dot{v}_{1}\left(2\Delta_{c1}\ddot{\Delta}_{c1}+\dot{\Delta}_{c1}^2\right)\right], \tag{25c}$$

the first of which has already been used (Eq. (18)) to evaluate Δ_{c1} (as in Eq. (19)) and $\dot{v}_{1c}=1$. With Δ_{c1} computed, the left members of all the successive perturbation equations vanish, so that, for compatibility, also the right members must be zero. Therefore, from the second equation, $\dot{\Delta}_{c1}=0$ is drawn. By taking the arbitrary quantity $\ddot{v}_{1c}=0$, compatibility of the third equation finally provides:

$$\ddot{\Delta}_{c1}=-\frac{2}{3\Delta_{c1}}. \tag{26}$$

With the previous results, coming back to the original variables, the bifurcated path $\mathcal{P}$ is described by the parametric equations:

$$u_1(\epsilon)=\frac{1}{2}\Delta(\epsilon)+\epsilon, \tag{27a}$$

$$\Delta(\epsilon)=\Delta_{c1}-\epsilon^2\frac{2}{3\Delta_{c1}}+O\left(\epsilon^3\right). \tag{27b}$$

If also the reactive force μ is of interest, it can be evaluated from the last of Eq. (7), as a function of the same parameter ϵ. Since displacements are expressed as power series of ϵ, the same occurs for the force, which assumes the form:

$$\mu=\mu_c+\epsilon\dot{\mu}_c+\epsilon^2\ddot{\mu}_c+O\left(\epsilon^3\right), \tag{28}$$

where (index 1 denotes evaluation on path $\mathcal{P}_1$):

$$\mu_{c1}=\frac{1}{4}\left[3(1+4\alpha)-\frac{1}{4}(1+16\beta)\Delta_{c1}^2\right]\Delta_{c1}\equiv\hat{\mu}\left(\Delta_{c1}\right), \tag{29a}$$

$$\dot{\mu}_{c1}=\frac{3}{8}\left[(1+8\beta)\Delta_{c1}^2-4(1+2\alpha)\right], \tag{29b}$$

$$\ddot{\mu}_{c1}=-\frac{4+16\alpha+(5+32\beta)\Delta_{c1}^2}{8\Delta_{c1}}. \tag{29c}$$

Three-mass chain. The perturbation Eq. (17) for the $n=3$ chain are governed by the matrix $\mathbf{K}_c$ in Eq. (20), and know terms $\ddot{\mathbf{f}}_c\left(\dot{\mathbf{v}},\dot{\Delta}_c\right)$, $\dddot{\mathbf{f}}_c\left(\dot{\mathbf{v}}_c,\ddot{\mathbf{v}}_c,\dot{\Delta}_c,\ddot{\Delta}_c\right)$ given in the Appendix B. By solving them in sequence, the following results are obtained:

- path $\mathcal{P}_1$:

$$\dot{\Delta}_{c1}=0,\qquad \ddot{\mathbf{v}}_{c1}=\left(-\ddot{v}_{c1},\ddot{v}_{c1}\right)^T, \tag{30a}$$

$$\ddot{\Delta}_{c1}=\frac{\alpha(2+27\beta(1+4\beta))+8\beta(2+9\beta)+1}{2(\alpha-4\beta)\sqrt{(1+3\alpha)(1+12\beta)}},\qquad \dddot{\mathbf{v}}_{c1}=(0,0)^T, \tag{30b}$$

where: $\ddot{v}_{c1}:=\frac{(1+6\beta)\sqrt{(1+3\alpha)(1+12\beta)}}{6(\alpha-4\beta)}$.

- path $\mathcal{P}_2$:

$$\dot{\Delta}_{c2}=\frac{3(1-2\beta)}{2(1+4\beta)},\qquad \ddot{\mathbf{v}}_{c2}=(0,0)^T, \tag{31a}$$

$$\ddot{\Delta}_{c2}=-\frac{9[1+4\beta(2+\beta)]}{8\sqrt{(1+\alpha)(1+4\beta)^3}},\qquad \dddot{\mathbf{v}}_{c2}=(0,0)^T. \tag{31b}$$

It is observed that the slope $\dot{\Delta}_{c1}$ of $\mathcal{P}_1$ is zero, so that one looks at the curvature, which is $\ddot{\Delta}_{c1}\gtrless 0$ when $\alpha\gtrless 4\beta$. Displacements along $\mathcal{P}_1$ change with Δ, in such a way $v_2(\epsilon)\gtrless v_1(\epsilon)$ when $\alpha\gtrless 4\beta$; moreover, the symmetric mode $m=1$ is changed by an antisymmetric correction. In contrast, the slope of $\mathcal{P}_2$ is $\dot{\Delta}_{c2}\gtrless 0$ when $\beta\lesseqgtr\frac{1}{2}$, a result which is expected to affects its stability. It is also interesting to note that the critical mode $m=2$ is not altered by nonlinearities (up-to the ϵ^3 order), so that the incremental displacements $v_1(\epsilon), v_2(\epsilon)$ remain equal and opposite while the control parameter Δ increases. Finally, note that the asymptotic expansion for $\mathcal{P}_1$ breaks down close to $\alpha=4\beta$.

With the previous results, coming back to the original variables, the bifurcated paths are expressed as follows:

- path $\mathcal{P}_1$:

$$\mathbf{u}(\epsilon)=\frac{1}{3}\Delta(\epsilon)\begin{pmatrix}1\\2\end{pmatrix}+\epsilon\begin{pmatrix}1\\1\end{pmatrix}+\epsilon^2\begin{pmatrix}-\frac{(1+6\beta)\sqrt{(1+3\alpha)(1+12\beta)}}{6(\alpha-4\beta)}\\ \frac{(1+6\beta)\sqrt{(1+3\alpha)(1+12\beta)}}{6(\alpha-4\beta)}\end{pmatrix}+O(\epsilon^4), \tag{32a}$$

$$\Delta(\epsilon)=3\sqrt{\frac{1+3\alpha}{1+12\beta}}+\epsilon^2\frac{\alpha(2+27\beta(1+4\beta))+8\beta(2+9\beta)+1}{2(\alpha-4\beta)\sqrt{(1+3\alpha)(1+12\beta)}}+O(\epsilon^3). \tag{32b}$$

- path $\mathcal{P}_2$:

$$\mathbf{u}(\epsilon)=\frac{1}{3}\Delta(\epsilon)\begin{pmatrix}1\\2\end{pmatrix}+\epsilon\begin{pmatrix}1\\-1\end{pmatrix}+O(\epsilon^4), \tag{33a}$$

$$\Delta(\epsilon)=3\sqrt{\frac{1+\alpha}{1+4\beta}}+\epsilon\frac{3(1-2\beta)}{2(1+4\beta)}-\epsilon^2\frac{9[1+4\beta(2+\beta)]}{8\sqrt{(1+\alpha)(1+4\beta)^3}}+O(\epsilon^3). \tag{33b}$$

Concerning the reactive force, it is expressed as in Eq. (28), with the following coefficients:

- path $\mathcal{P}_1$:

$$\mu_{c1}=\frac{9\alpha+20\beta+96\alpha\beta+2}{2}\sqrt{\frac{1+3\alpha}{(1+12\beta)^3}}, \tag{34a}$$

$$\dot{\mu}_{c1}=0, \tag{34b}$$

$$\ddot{\mu}_{c1}=-\frac{1620\alpha\beta^2+261\alpha\beta+10\alpha+504\beta^2+80\beta+3}{4\sqrt{(1+3\alpha)(1+12\beta)^3}}. \tag{34c}$$

- path $\mathcal{P}_2$:

$$\mu_{c2}=\frac{11\alpha-4\beta+32\alpha\beta+2}{2}\sqrt{\frac{1+\alpha}{(1+4\beta)^3}}, \tag{35a}$$

$$\dot{\mu}_{c2}=\frac{9(1-2\beta)(\alpha-4\beta)}{4(1+4\beta)^2}, \tag{35b}$$

$$\ddot{\mu}_{c2}=-\frac{27\left[\alpha\left(128\beta^3+76\beta^2+32\beta+3\right)+112\beta^3+40\beta^2+20\beta+2\right]}{16\sqrt{(1+\alpha)(1+4\beta)^5}}. \tag{35c}$$

It is noticed that the slope $\dot{\mu}_{c1}$ of $\mathcal{P}_1$ is zero, and the curvature $\ddot{\mu}_{c1}$ always negative; the sign of the slope $\dot{\mu}_{c2}$ of $\mathcal{P}_2$, depends both on $\alpha\gtrless 4\beta$ and $\beta\gtrless\frac{1}{2}$.

Four-mass chain. The stiffness matrix of the $n=4$ chain appears in Eq. (22) with know terms given in Appendix B. By performing analogous steps, the results listed below are drawn.

- path $\mathcal{P}_1$:

$$\mathbf{u}(\epsilon)=\frac{1}{4}\Delta(\epsilon)\begin{pmatrix}1\\2\\3\end{pmatrix}+\epsilon\begin{pmatrix}\frac{\sqrt{2}}{2}\\1\\\frac{\sqrt{2}}{2}\end{pmatrix}+\epsilon^2\Delta_{c1}\begin{pmatrix}\frac{\left(1-\sqrt{2}-4\beta\right)\left(32\beta^2+16\beta+1\right)}{8(\alpha-4\beta)\left[8\left(\sqrt{2}-1\right)\beta+\sqrt{2}\right]}\\0\\-\frac{\left(1-\sqrt{2}-4\beta\right)\left(32\beta^2+16\beta+1\right)}{8(\alpha-4\beta)\left[8\left(\sqrt{2}-1\right)\beta+\sqrt{2}\right]}\end{pmatrix}+O(\epsilon^3), \tag{36a}$$

$$\Delta(\epsilon)=\Delta_{c1}+\frac{\epsilon^2}{\Delta_{c1}}\left(\frac{4\left\{\alpha\left[4\left(\sqrt{2}+1\right)\beta+2\right]+\sqrt{2}-1\right\}}{\alpha-4\beta}+\frac{4\left(27\sqrt{2}-38\right)\beta+8\sqrt{2}-11}{32\beta^2+16\beta+1}-2\sqrt{2}-1\right)+O(\epsilon^3), \tag{36b}$$

with Δ_{c1} in Eq. (24).

- path $\mathcal{P}_2$:

$$\mathbf{u}(\epsilon)=\frac{1}{4}\Delta(\epsilon)\begin{pmatrix}1\\2\\3\end{pmatrix}+\epsilon\begin{pmatrix}1\\0\\-1\end{pmatrix}+O(\epsilon^3), \tag{37a}$$

$$\Delta(\epsilon)=\Delta_{c2}-\epsilon^2\frac{8}{3\Delta_{c2}}+O(\epsilon^3), \tag{37b}$$

with Δ_{c2} in Eq. (24).

- path $\mathcal{P}_3$:

$$\mathbf{u}(\epsilon)=\frac{1}{4}\Delta(\epsilon)\begin{pmatrix}1\\2\\3\end{pmatrix}+\epsilon\begin{pmatrix}\frac{\sqrt{2}}{2}\\-1\\\frac{\sqrt{2}}{2}\end{pmatrix}+\epsilon^2\Delta_{c3}\begin{pmatrix}-\frac{\left(1+\sqrt{2}-4\beta\right)\left(32\beta^2+16\beta+1\right)}{8(\alpha-4\beta)\left[8\left(\sqrt{2}+1\right)\beta+\sqrt{2}\right]}\\0\\\frac{\left(1+\sqrt{2}-4\beta\right)\left(32\beta^2+16\beta+1\right)}{8(\alpha-4\beta)\left[8\left(\sqrt{2}+1\right)\beta+\sqrt{2}\right]}\end{pmatrix}+O(\epsilon^3), \tag{38a}$$

$$\Delta(\epsilon)=\Delta_{c3}-\frac{\epsilon^2}{\Delta_{c3}}\left(\frac{4\left\{\left(\alpha\left[4\left(\sqrt{2}-1\right)\beta-2\right]+\sqrt{2}+1\right)\right\}}{\alpha-4\beta}+\frac{4\left(27\sqrt{2}+38\right)\beta+8\sqrt{2}+11}{32\beta^2+16\beta+1}-2\sqrt{2}+1\right)+O(\epsilon^3), \tag{38b}$$

with Δ_{c3} defined in Eq. (24).

It is worth noticing that $\dot{\Delta}_{cm}=0$ for any paths. Moreover, while the antisymmetric pattern of the buckling mode $m=2$ is unaffected by nonlinearities (to within the truncated order analysis), the symmetric buckling modes $m=1,3$ are instead corrected by antisymmetric displacements induced by the variation of the control parameter Δ.

The expressions for the reactive forces are omitted for brevity.

4. Secondary bifurcations

A bifurcation analysis is carried out along each path $\mathcal{P}_1,\dots,\mathcal{P}_{n-1}$ branching from $\mathcal{F}$, to detect the possible occurrence of further (*secondary*, or successive) bifurcations (see Fig. 2).

A bifurcated path $\mathcal{P}_m$ is known in the parametric form $\mathbf{u}=\mathbf{u}(\epsilon)$, $\Delta=\Delta(\epsilon)$, as expressed by Eq. (27) for the two-mass chain, Eqs. (32), (33) for the three-mass chain, and Eqs. (36)–(38) for the four-mass chain. To detect a secondary bifurcation points B_m (possibly more than one) along it, and to build-up the secondary bifurcated paths S_m emanating from it, incremental displacements $\mathbf{w}$ are introduced, measured from $\mathcal{P}_m$, i.e.:

$$\mathbf{u}=\mathbf{u}(\epsilon)+\mathbf{w}. \tag{39}$$

The secondary bifurcated path is sought in the parametric form $\mathbf{w} = \mathbf{w}(s)$, $\epsilon = \epsilon(s)$, with s a new parameter, vanishing at C_m, and then expanded as [23]:

$$\mathbf{w}(s) = s\mathbf{w}_b' + s^2\mathbf{w}_b'' + \cdots, \tag{40a}$$

$$\epsilon(s) = \epsilon_b + s\epsilon_b' + s^2\epsilon_b'' + \cdots, \tag{40b}$$

where $q_b' := \left.\frac{\mathrm{d}q}{\mathrm{d}s}\right|_{s=0}$, $q_b'' := \left.\frac{1}{2}\frac{\mathrm{d}^2q}{\mathrm{d}s^2}\right|_{s=0}$, $q_b''' := \left.\frac{1}{6}\frac{\mathrm{d}^3q}{\mathrm{d}s^3}\right|_{s=0}$, for any magnitude $q = q(s)$ on the path; moreover, ϵ_b is the (unknown) value of ϵ selecting B_m along $\mathcal{P}_m$. By using the series expressions within Eq. (40) in the $n-1$ equilibrium Eq. (14), a sequence of equations similar to Eq. (17) is obtained. By solving them in cascade, the unknowns $(\epsilon_b, \mathbf{w}_b'; \epsilon_b', \mathbf{w}_b''; \cdots)$ are evaluated, able to describe the secondary path(s). However, owing to the complexity of algebra, we renounce to such a cumbersome analysis, and confine ourselves to determine the secondary bifurcation point at ϵ_b, by postponing the construction of the path to the numerical analysis. In this regard, the power of the asymptotic analysis is fully exploited, in detecting the qualitative character of the solution, and in guiding the successive numerical analysis.

Accordingly, just the s^1 order perturbation equation is computed, having the following form:

$$\mathbf{K}|_{\mathcal{P}_m}(\epsilon_b)\,\mathbf{w}_b' = \mathbf{0}, \tag{41}$$

where $\mathbf{K}|_{\mathcal{P}_m}(\epsilon_b)$ is the tangent stiffness matrix to $\mathcal{P}_m$ at B_m. The non-trivial roots of the characteristic equation $\det\left[\mathbf{K}|_{\mathcal{P}_m}(\epsilon_b)\right] = 0$ are the critical values sought (since the trivial solution $\epsilon_b = 0$ reproduces the bifurcation at C_m).

Referring to the generic point ϵ on $\mathcal{P}_m$ (in order to build-up expressions of $\mathbf{K}|_{\mathcal{P}_m}(\epsilon)$ useful also for the successive stability analysis), we observe that, since $\mathbf{K}|_{\mathcal{P}_m}(\epsilon)$ is a polynomial function of ϵ, and the paths $\mathcal{P}_m$ are expressed to within an error of order (ϵ^3), it must be taken for consistency:

$$\mathbf{K}|_{\mathcal{P}_m}(\epsilon) = \mathbf{K}_{cm} + \epsilon\dot{\mathbf{K}}_{cm} + \epsilon^2\ddot{\mathbf{K}}_{cm} + O\left(\epsilon^3\right), \tag{42}$$

where $\mathbf{K}_{cm} = \mathbf{K}|_{\mathcal{P}_m}(0)$ is the stiffness matrix evaluated at the primary bifurcation point C_m (i.e., the matrix $\mathbf{K}_c$ appearing in Eq. (17) evaluated for each critical value Δ_{cm}), and $\dot{\mathbf{K}}_{cm}$, $\ddot{\mathbf{K}}_{cm}$ are the derivatives of $\mathbf{K}|_{\mathcal{P}_m}(\epsilon)$ with respect to ϵ, evaluated at C_m.

To simplify the analysis, the following strategy is adopted: (a) if the first-order perturbation $\dot{\mathbf{K}}_{cm}$ gives a non-trivial answer, i.e., a non-zero root ϵ_b is found, then the analysis is truncated at this order; (b) if such a lower-order approximation gives no significant roots, then the second-order approximation $\ddot{\mathbf{K}}_{cm}$ is accounted for. For the three chains analyzed, we find the following results.

Two-mass chain. The stiffness matrix of the two-masses chain is given by Eq. (A.5). To compute it at a generic point of $\mathcal{P}_1$, the parametric equations $u_1 = u_1(\epsilon)$, $\Delta = \Delta(\epsilon)$ in Eq. (27) must be substituted in it, and terms up-to ϵ^2 retained. It follows, that

$$\mathbf{K}|_{\mathcal{P}_1}(\epsilon) = \left[-\frac{4}{3}(1+8\beta)\epsilon^2\right]. \tag{43}$$

Since $\det\left[\mathbf{K}(\epsilon_b)|_{\mathcal{P}}\right] = 0$ admits only the trivial root $\epsilon_b = 0$, it follows that the primary bifurcated path $\mathcal{P}_1$ does not post-bifurcate.

Three-mass chain. The stiffness matrix of the three-masses chain is given by Eq. (A.6). To evaluate it at a generic point of $\mathcal{P}_{1,2}$, the parametric equations $u_i = u_i(\epsilon)$, $\Delta = \Delta(\epsilon)$ in Eqs. (32) or (33) must be substituted in the matrix, and terms up-to ϵ^2 retained. We obtain the results reported below.

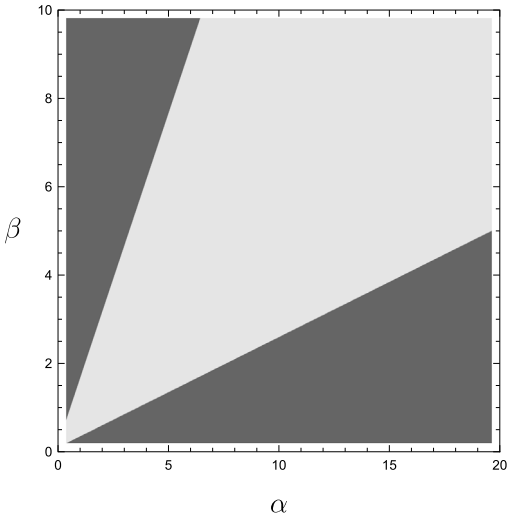

Fig. 3. Map of the real roots of the post-bifurcation condition in Eq. (45), relevant to $\mathcal{P}_1$. The regions corresponding to zero or two post-bifurcated paths are shaded in light gray and dark gray, respectively.

Path $\mathcal{P}_1$ The stiffness matrix in Eq. (42) reads:

$$\mathbf{K}|_{\mathcal{P}_1}(\epsilon) = \frac{3(\alpha-4\beta)}{1+12\beta}\begin{bmatrix}-1 & 1\\ 1 & -1\end{bmatrix} - \frac{2}{3}\epsilon(1+6\beta)\Delta_{c1}\begin{bmatrix}1 & 0\\ 0 & -1\end{bmatrix} + \epsilon^2\begin{bmatrix}\frac{1}{12}\left(5(9\alpha+2)-72\beta-\frac{2}{1+12\beta}\right. & \frac{\alpha(135\beta(4\beta+1)+8)}{3(12\beta+1)(\alpha-4\beta)}\\ \left.-\frac{3(3\alpha+2)(5\alpha+2)}{\alpha-4\beta}\right) & +\frac{4\beta(54\beta+13)+3}{3(12\beta+1)(\alpha-4\beta)}\\ \frac{\alpha(135\beta(4\beta+1)+8)}{3(12\beta+1)(\alpha-4\beta)} & \frac{1}{12}\left(5(9\alpha+2)-72\beta-\frac{2}{1+12\beta}\right.\\ +\frac{4\beta(54\beta+13)+3}{3(12\beta+1)(\alpha-4\beta)} & \left.-\frac{3(3\alpha+2)(5\alpha+2)}{\alpha-4\beta}\right)\end{bmatrix} + O(\epsilon^3), \tag{44}$$

where also second-order terms were retained. Indeed, if the matrix were truncated at the first order, $\mathbf{K}|_{\mathcal{P}_1}(\epsilon) = 0$ would provide only the double root $\epsilon_{b1} = 0$. By including also the second-order terms:

$$\epsilon_{b1} = \pm\sqrt{\frac{3(\alpha-4\beta)(1+2\alpha+16\beta+27\alpha\beta+72\beta^2+108\alpha\beta^2)}{(1+9\beta)\left[1+16\beta+44\beta^2-144\beta^3+\alpha\left(216\beta^2+52\beta+3\right)\right]}}, \tag{45}$$

and $\epsilon_{b1} = 0$ is found again. The roots of Eq. (45) are reals when $\alpha > 4\beta$ or when:

$$\alpha < \frac{144\beta^3-44\beta^2-16\beta-1}{216\beta^2+52\beta+3}. \tag{46}$$

The region of existence of the roots on the (α,β)-plane, which correspond to two post-bifurcated paths, are displayed in Fig. 3.

Path $\mathcal{P}_2$ The stiffness matrix in Eq. (42) reads:

$$\mathbf{K}|_{\mathcal{P}_2}(\epsilon) = \frac{\alpha-4\beta}{1+4\beta}\begin{bmatrix}1 & 1\\ 1 & 1\end{bmatrix} - \epsilon\frac{\Delta_{c2}}{1+4\beta}\begin{bmatrix}4\beta(1+2\beta) & 1+6\beta\\ 1+6\beta & 4\beta(1+2\beta)\end{bmatrix} + O\left(\epsilon^2\right), \tag{47}$$

in which we neglected $O(\epsilon^2)$ terms. By taking $\epsilon = \epsilon_{b2}$ and solving $\det\left[\mathbf{K}|_{\mathcal{P}_2}(\epsilon_{b2})\right] = 0$, we find the nontrivial solution:

$$\epsilon_{b2} = \frac{2(\alpha-4\beta)}{\Delta_{c2}\left(1+10\beta+8\beta^2\right)}. \tag{48}$$

Hence, $\epsilon_{b2} \gtrless 0$ according to $\alpha \gtrless 4\beta$. Therefore, just one secondary bifurcation point B_2 exists along $\mathcal{P}_2$. It should be noticed that the distance between C_2 and B_2 is proportional to the difference $\alpha - 4\beta$. Thus, when the degenerate case $\alpha = 4\beta$ is approached, secondary and

$$\mathbf{K}_{cm} = \frac{\alpha - 4\beta}{32\beta^2 + 16\beta + 1}\begin{bmatrix} 4\left(2 \mp 3\sqrt{2}\right)\beta \mp 2\sqrt{2} - 1 & 8\beta \pm \sqrt{2} + 2 & -1 \pm 4\left(\sqrt{2} \mp 2\right)\beta \\ & \mp 2\left(4\sqrt{2}\beta + \sqrt{2} \pm 1\right) & 8\beta + 2 \pm \sqrt{2} \\ \text{SYM} & & 4\left(2 \mp 3\sqrt{2}\right)\beta \mp 2\sqrt{2} - 1 \end{bmatrix}, \tag{51}$$

$$\dot{\mathbf{K}}_{cm} = 4\sqrt{\frac{1 + \left(2 \pm \sqrt{2}\right)\alpha}{1 + \left(2 \pm \sqrt{2}\right)4\beta}}\begin{bmatrix} \mp\frac{1}{2} - 2\sqrt{2}\beta & \pm\frac{1}{4}\left(2 \mp \sqrt{2}\right) & 0 \\ & 0 & \frac{1}{4}\left(\sqrt{2} \mp 2\right) \\ \text{SYM} & & \pm\frac{1}{2} + 2\sqrt{2}\beta \end{bmatrix}, \tag{52}$$

$$\ddot{\mathbf{K}}_{cm} = \begin{bmatrix} \pm\sqrt{2} - 2 - \frac{\Delta_{cm}\ddot{\Delta}_{cm}}{4} & \frac{3}{2} \mp \sqrt{2} & \frac{1}{2}\beta\Delta_{cm}(\ddot{\Delta}_{cm} \mp 4\ddot{v}_{mc}) \\ +\beta\left(-\frac{3\Delta_{cm}\ddot{\Delta}_{cm}}{2} \mp 2\Delta_{cm}\ddot{v}_{mc} - 4\right) & +\frac{\Delta_{cm}}{8}\left(\ddot{\Delta}_{cm} \mp 4\ddot{v}_{mc}\right) & \\ & \pm 2\sqrt{2} - 3 - \beta(\Delta_{cm}\ddot{\Delta}_{cm} + 2) & \frac{3}{2} \mp \sqrt{2} + \frac{1}{8}\Delta_{cm}(\ddot{\Delta}_{cm} \mp 4\ddot{v}_{mc}) \\ & -\frac{\Delta_{cm}\ddot{\Delta}_{cm}}{4} \pm \Delta_{cm}\ddot{v}_{mc} & \\ & & \pm\sqrt{2} - 2 - \frac{\Delta_{cm}\ddot{\Delta}_{cm}}{4} \\ \text{SYM} & & +\beta\left(-\frac{3\Delta_{cm}\ddot{\Delta}_{cm}}{2} \mp 2\Delta_{cm}\ddot{v}_{mc} - 4\right) \end{bmatrix}. \tag{53}$$

Box I.

primary bifurcation points tend to coalesce (similarly to what happens in the Augusti model [23]).

The critical mode is $\mathbf{w}'_{b2} = (1,1)^T$, which the projection of the tangent to $\mathcal{S}_2$ at B_2 onto the (u_1, u_2) plane, an information useful for a numerical search of the post-bifurcated path. It is observed that $\mathcal{P}_2$, along which the deflection is antisymmetric, post-bifurcates in a symmetric pattern. The total elongation corresponding to ϵ_{b2}, by the way of Eq. (33), turns out to be:

$$\Delta_{b2} = 3\sqrt{\frac{1+\alpha}{1+4\beta}} + \epsilon_{b2}\frac{3(1-2\beta)}{2(1+4\beta)} + O\left(\epsilon_{b2}^2\right). \tag{49}$$

The load at the same point is evaluated by the last of Eq. (33):

$$\mu_{b2} = \frac{11\alpha - 4\beta + 32\alpha\beta + 2}{2}\sqrt{\frac{1+\alpha}{(1+4\beta)^3}} + \epsilon_{b2}\frac{9(1-2\beta)(\alpha-4\beta)}{4(1+4\beta)^2} + O\left(\epsilon_{b2}^2\right). \tag{50}$$

Four-mass chain. The stiffness matrix of the four-masses chain is given in Eq. (A.7). When the matrix is computed at a generic point of $\mathcal{P}_{1,2,3}$, the parametric equations $u_i = u_i(\epsilon)$, $\Delta = \Delta(\epsilon)$, given in Eqs. (36)–(38), respectively, must be substituted in the matrix, and terms up-to ϵ^2 retained. It has been checked that, if terms of ϵ^2 order were neglected, only the trivial solution $\epsilon_b = 0$ would be found. For the different paths, we obtain the results reported below.

Paths $\mathcal{P}_{1,3}$ The matrices in Eq. (42) ($m = 1, 3$) assume the form shown in Eqs. (51) to (53) in Box I, with Δ_{cm} ($m = 1, 3$) defined in Eq. (24), and $\ddot{\Delta}_{cm}$, $\ddot{v}_{c2m}$ appearing in Eqs. (36) ($m = 1$) and (38) ($m = 3$). The relevant eigenvalue problem leads to a sixth-degree characteristic equation of the type:

$$\left[\epsilon_{bm}^4 + f_m(\alpha,\beta)\epsilon_{bm}^2 + g_m(\alpha,\beta)\right]\epsilon_{bm}^2 = 0, \tag{54}$$

where $f_m(\cdot), g_m(\cdot)$ are not reported for brevity. Eq. (54) admits the double root $\epsilon_{bm} = 0$; moreover, it admits two, one or zero positive roots ϵ_{bm}^2, according to the values of α, β. A discussion of the roots of the bi-quadratic equation, leads to the maps in Fig. 4, in which the regions of existence of the roots are displayed on the (α, β)-plane. When no roots $\epsilon_{bm}^2 > 0$ exist for Eq. (54), the path $\mathcal{P}_m$ does not post-bifurcate. When just one root $\epsilon_{bm}^2 > 0$ exists, *two* secondary bifurcation points $B_m^{\pm}$ appear along $\mathcal{P}_m$, at $\epsilon_{bm}^{\pm} := \pm\sqrt{\epsilon_{bm}^2}$, respectful of the symmetry of the paths. When two roots $\epsilon_{bm,1}^2, \epsilon_{bm,2}^2 > 0$ exist, *four* secondary bifurcations points $B_{m,k}^{\pm}$ ($k = 1, 2$) occur on $\mathcal{P}_m$, at $\epsilon_{bm,k}^{\pm} := \pm\sqrt{\epsilon_{bm,k}^2}$.

Since at the post-bifurcation point the stiffness matrix does not possess any reflection symmetry (since the entries $(1,1)$ and $(3,3)$ are equal in $\mathbf{K}_{cm}, \ddot{\mathbf{K}}_{cm}$, but opposite in $\dot{\mathbf{K}}_{cm}$), the buckling modes $\mathbf{w}'_{bm}$ are neither symmetric nor antisymmetric. Once ϵ_{bm} has been computed, the relevant total elongations and load are evaluated by Eq. (36) or (38).

Path $\mathcal{P}_2$ The matrices in Eq. (42) assume the form:

$$\mathbf{K}_{c2} = \frac{\alpha - 4\beta}{1 + 8\beta}\begin{bmatrix} -1 & 2 & -1 \\ & -2 & 2 \\ \text{SYM} & & -1 \end{bmatrix},$$
$$\dot{\mathbf{K}}_{c2} = 4\sqrt{\frac{1+2\alpha}{1+8\beta}}\begin{bmatrix} -2\beta & -\frac{1}{2} & -2\beta \\ & 1 & -\frac{1}{2} \\ \text{SYM} & & -2\beta \end{bmatrix}, \tag{55}$$
$$\ddot{\mathbf{K}}_{c2} = \frac{2}{3}\begin{bmatrix} -2(1+6\beta) & 1 & 4\beta \\ & -2(1-2\beta) & 1 \\ \text{SYM} & & -2(1+6\beta) \end{bmatrix}. \tag{56}$$

The relevant characteristic equation is:

$$\left[c_0\epsilon_{b2}^4 + c_1\epsilon_{b2}^3 + c_2\epsilon_{b2}^2 + c_3\epsilon_{b2} + c_4\right]\epsilon_{b2}^2 = 0, \tag{57}$$

where:

$$c_0 := 4\beta^2 - \beta - \frac{1}{4}, \qquad c_1 := 12\beta^2\sqrt{\frac{1+2\alpha}{1+8\beta}},$$
$$c_2 := \frac{3(\alpha(46\beta+6) + 8\beta(\beta+3) + 3)}{32\beta + 4}, \tag{58}$$
$$c_3 := -\frac{9(\alpha-4\beta)(1+4\beta)}{32\beta+4}\sqrt{\frac{1+2\alpha}{1+8\beta}}, \qquad c_4 := \frac{9(\alpha-4\beta)^2}{8(1+8\beta)^2}.$$

Again, a double zero root is found; moreover, there exist zero, two or four real roots $\epsilon_{b2,k}$, to each of which a secondary bifurcation point $B_{2,k}$ is associated.

Since the discussion of the complete quartic equation is not easy, as an attempt to factorize the equation, the invariance property of $\mathbf{K}|_{\mathcal{P}_2}(\epsilon)$ with respect the exchange $w'_{b1} \leftrightarrow w'_{b3}$ was exploited. Accordingly, the eigenvalue problem in Eq. (41) was split in two sub-problems, i.e.: (a) the antisymmetric problem, in which $w'_{b3} = -w'_{b1}$, $w'_{b2} = 0$, and (b) the symmetric problem, in which $w'_{b3} = w'_{b1}$. By denoting by $k_{ij}(\epsilon_b)$ the components of $\mathbf{K}|_{\mathcal{P}_2}(\epsilon_b)$, the two sub problems read:

$$\left[k_{11}(\epsilon_b) - k_{13}(\epsilon_b)\right]w'_{b1} = 0, \tag{59a}$$
$$\begin{bmatrix} 2\left[k_{11}(\epsilon_b) + k_{13}(\epsilon_b)\right] & 2k_{12}(\epsilon_b) \\ 2k_{12}(\epsilon_b) & k_{22}(\epsilon_b) \end{bmatrix}\begin{pmatrix} w'_{b1} \\ w'_{b2} \end{pmatrix} = \begin{pmatrix} 0 \\ 0 \end{pmatrix}, \tag{59b}$$

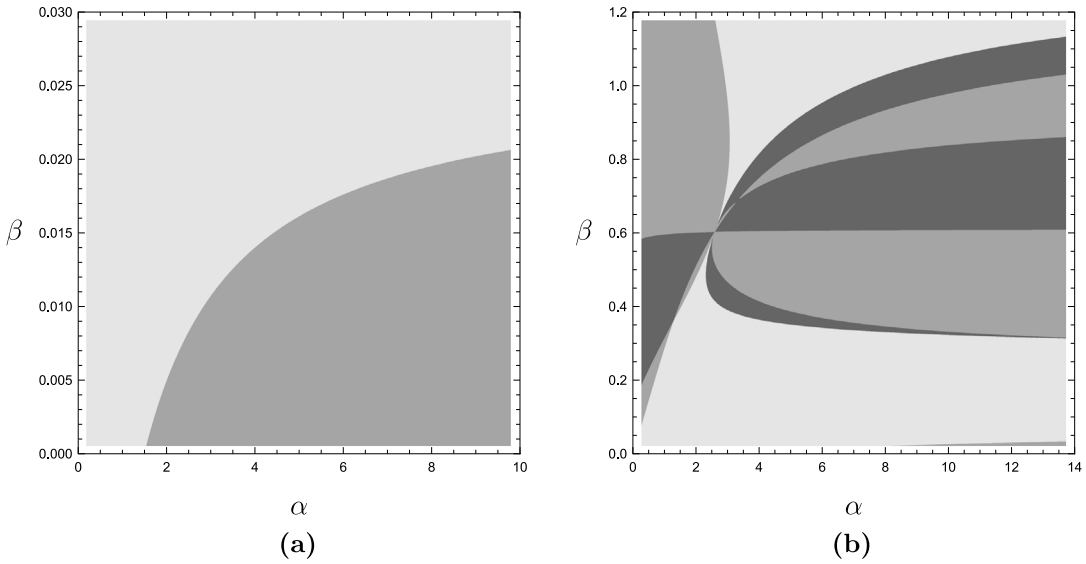

Fig. 4. Map of the positive roots of the post-bifurcation condition in Eq. (54), for: (a) path $\mathcal{P}_1$, (b) path $\mathcal{P}_3$. Zero, one or two positive roots denote the existence of zero, two or four post-bifurcated paths, with the corresponding regions indicated in light, medium, and dark gray, respectively.

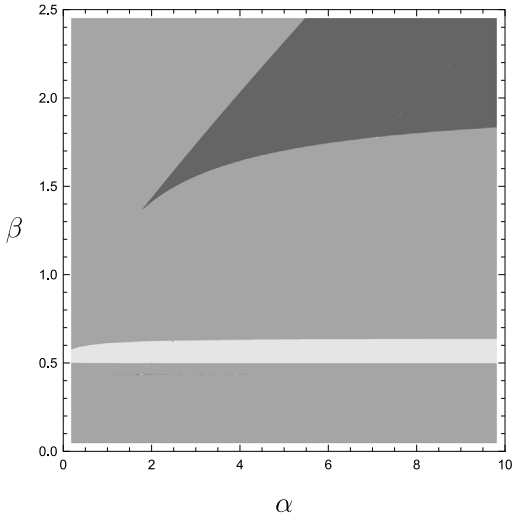

Fig. 5. Map of the real roots of the post-bifurcation condition Eq. (57), relevant to $\mathcal{P}_2$, revealing the existence of zero, two or four post-bifurcated paths, with the corresponding regions indicated in light, medium, and dark gray, respectively.

the first of which being quadratic and the second quartic in the unknown ϵ_b. Unfortunately, the antisymmetric problem only admits the double zero root, so that the symmetric problem returns the quartic characteristic equation of the whole problem. However, although unsuccessful, the attempt gave us the information that $\mathcal{P}_2$ (along which the deflection $\mathbf{v}_c$ is antisymmetric) post-bifurcates (if it does) by a symmetric mode $\mathbf{w}_c'$. The quartic algebraic equation is discussed in Appendix C; the relevant results are represented in Fig. 5, where a map identifies the regions of the (α, β) plane, in which the number of the real roots is indicated.

5. Stability analysis

The stability of the equilibrium paths of the chain is ascertained by the Lagrange–Dirichlet theorem. This states that an equilibrium point of a conservative system is stable if the TPE is positive definite, i.e., if its Hessian matrix possesses all positive eigenvalues. Expressed the path under study in the parametric form $u_i = u_i(\epsilon)\ \left(i = 1, \dots, u_{n-1}\right)$, $\Delta = \Delta(\epsilon)$, the Hessian matrix $\mathbf{K}(\epsilon) := \left[\frac{\partial^2 W(\epsilon)}{\partial u_i \partial u_j}\right]$ coincides with the tangent stiffness matrix to the path at the point of abscissa ϵ. Its (all real) eigenvalues $\lambda_j(\epsilon)$ are the roots of the characteristic equation $\det\left[\mathbf{K}(\epsilon) - \lambda(\epsilon)\mathbf{I}\right] = 0$. If all λ_j are positive, then the equilibrium point at ϵ is stable; if even just one of the eigenvalues is negative, the equilibrium is there unstable.

It is worth stressing that we are studying the stability of equilibrium points existing in (quasi-static) displacement-controlled loading processes. This entails that *no limit points occur* along the fundamental path, so that stability can only be lost via a branching point. If, in contrast, force-controlled loadings are also of interest, the further loss of stability at the limit point L must be accounted for. The topic is tackled more in-depth in the Appendix D.

Two-mass chain. The stiffness matrix of the two-mass chain is expressed by Eq. (A.5). To evaluate this matrix on the fundamental path $\mathcal{F}$, $\epsilon = \Delta$ must be used as parameter and displacements replaced from Eq. (11) (for $n = 2$), to obtain:

$$\mathbf{K}|_{\mathcal{F}}(\Delta) = \left[2 + 4\alpha - \frac{1}{2}(1 + 8\beta)\Delta^2\right], \tag{60}$$

(i.e., the matrix in Eq. (18), but evaluated at a generic Δ, instead of Δ_{c1}). This 1×1 matrix is definite positive when $\Delta < \Delta_{c1}$, and definite negative when $\Delta > \Delta_{c1}$. Therefore, $\mathcal{F}$ loses stability at the bifurcation point C_1 and remains unstable above it.

To evaluate stability of the bifurcated path $\mathcal{P}_1$, the stiffness matrix in Eq. (43) must by examined. Since it is negative definite for any ϵ, the primary bifurcated path is unstable, irrespective of $\alpha \lessgtr 4\beta$.

Three-mass chain. The stiffness matrix of the three-mass chain is given by Eq. (A.6). Using $\epsilon = \Delta$ as parameter and displacements expressed by Eq. (11) (with $n = 3$), the stiffness matrix evaluated on the fundamental path $\mathcal{F}$ is expressed by:

$$\mathbf{K}|_{\mathcal{F}}(\Delta) = \begin{bmatrix} 2 + 3\alpha - \frac{1}{3}\left(\frac{2}{3} + 4\beta\right)\Delta^2 & -1 + \frac{\Delta^2}{9} \\ -1 + \frac{\Delta^2}{9} & 2 + 3\alpha - \frac{1}{3}\left(\frac{2}{3} + 4\beta\right)\Delta^2 \end{bmatrix}, \tag{61}$$

(which coincides with the matrix $\mathbf{K}_c$ in Eq. (20), evaluated at a generic Δ, instead of Δ_{cm}). Its eigenvalues are:

$$\lambda_1(\Delta) = 3 + 3\alpha - \frac{1}{3}(1 + 4\beta)\Delta^2, \tag{62a}$$

$$\lambda_2(\Delta) = 1 + 3\alpha - \frac{1}{9}(1 + 12\beta)\Delta^2. \tag{62b}$$

By remembering the definitions of the critical values Δ_{cm} in Eq. (21), it follows that $\lambda_m = 0$ at $\Delta = \Delta_{cm}$, $m = 1, 2$. Since both eigenvalues $\lambda_m(\Delta)$ monotonically decrease with Δ, starting from a positive value, it happens than once the smallest of them vanishes (i.e., λ_1 when $\alpha < 4\beta$ and λ_2 when $\alpha > 4\beta$), stability is lost along the fundamental path, and not regained along this path. Therefore, $\mathcal{F}$ is stable below the first bifurcation point and unstable above.

The stability of the paths $\mathcal{P}_{1,2}$, is governed by the stiffnesses matrices $\mathbf{K}|_{\mathcal{P}_{1,2}}(\epsilon)$ in Eqs. (47), (44), respectively. The eigenvalues of $\mathbf{K}|_{\mathcal{P}_1}$ are roots of:

$$\lambda^2 + \left(\frac{6(\alpha - 4\beta)}{1 + 12\beta} + O\left(\epsilon^2\right)\right)\lambda - \frac{4\{\alpha[27\beta(1 + 4\beta) + 2] + 1 + 8\beta(2 + 9\beta)\}}{1 + 12\beta}\epsilon^2 + O\left(\epsilon^3\right) = 0. \tag{63}$$

Since the known term of this equation is negative, then $\lambda_1\lambda_2 < 0$, i.e., $\mathcal{P}_1$ is unstable (close to C_1).

The eigenvalues of $\mathbf{K}|_{\mathcal{P}_2}$ are:

$$\lambda_1(\epsilon) = \frac{1}{1 + 4\beta}\left[2(\alpha - 4\beta) - \left(1 + 10\beta + 8\beta^2\right)\epsilon\Delta_{c2}\right], \tag{64a}$$

$$\lambda_2(\epsilon) = (1 - 2\beta)\epsilon\Delta_{c2}, \tag{64b}$$

from which it follows:

- for $\epsilon > 0$:
  - if $\alpha > 4\beta$ and $\beta < \frac{1}{2}$, $\mathcal{P}_2$ is stable up to $\epsilon < \epsilon_b$, with ϵ_b given in Eq. (48), i.e., before the post-bifurcation occurs at B_2;
  - otherwise $\mathcal{P}_2$ is unstable;
- for $\epsilon < 0$:
  - if $\alpha > 4\beta$ and $\beta > \frac{1}{2}$, $\mathcal{P}_2$ is stable;
  - if $\alpha < 4\beta$ and $\beta > \frac{1}{2}$, $\mathcal{P}_2$ is stable for $\epsilon < \epsilon_b$, with ϵ_b given in Eq. (48), i.e., after the post-bifurcation occurs at B_2;
  - otherwise $\mathcal{P}_2$ is unstable.

In conclusion, the chain loses stability at the lower bifurcation point. In the post-critical range with $\epsilon > 0$, it can regain stability along the lowest bifurcated path only if $\alpha > 4\beta$ and $\beta < \frac{1}{2}$. However, even under these favorable conditions, the chain loses stability again at the secondary bifurcation point B_2. For $\epsilon < 0$, the chain is stable when $\alpha > 4\beta$ and $\beta > \frac{1}{2}$, or it can regain stability along the bifurcated path $\mathcal{P}_2$ when $\alpha < 4\beta$ and $\beta > \frac{1}{2}$, after the post-bifurcation occurs at B_2.

Four-mass chain. The stiffness matrix of the four-mass chain is given by Eq. (A.7). On the fundamental path $\mathcal{F}$, $\epsilon = \Delta$ is taken and displacements expressed by Eq. (11) (with $n = 4$); consequently:

$$\mathbf{K}|_{\mathcal{F}}(\Delta) = \begin{bmatrix} 2 + 3\alpha - \frac{1}{8}(6\beta + 1)\Delta^2 & \frac{\Delta^2}{16} - 1 & \frac{\beta\Delta^2}{4} - \alpha \\ & 2(1 + \alpha) - \frac{1}{8}(4\beta + 1)\Delta^2 & \frac{\Delta^2}{16} - 1 \\ \text{SYM} & & 2 + 3\alpha - \frac{1}{8}(6\beta + 1)\Delta^2 \end{bmatrix}, \tag{65}$$

whose eigenvalues are:

$$\lambda_1(\Delta) = 2 - \sqrt{2} + 2\alpha - \frac{1}{16}\left(2 - \sqrt{2} + 8\beta\right)\Delta^2, \tag{66a}$$

$$\lambda_2(\Delta) = 2 + 4\alpha - \frac{1}{8}(1 + 8\beta)\Delta^2, \tag{66b}$$

$$\lambda_3(\Delta) = 2 + \sqrt{2} + 2\alpha - \frac{1}{16}\left(2 + \sqrt{2} + 8\beta\right)\Delta^2. \tag{66c}$$

For this case, a discussion entirely analogous to that made for the system with three masses applies. Therefore, $\mathcal{F}$ is stable below the first bifurcation point and unstable above.

Finally, regarding the stability analysis of bifurcated paths, due to the complexity of the algebra involved, it is more convenient to proceed numerically. However, such an analysis is omitted here, for the sake of brevity.

6. Numerical results

The asymptotic results derived in the preceding sections are here compared with purely numerical analyses (carried out by the software Wolfram Mathematica [24]) to assess their validity. Specifically, for each of the configurations with two, three, or four masses, two case studies were examined: the first with $\alpha = 16$ and $\beta = 0.1$, falling under the condition $\alpha > 4\beta$, and the second with $\alpha = 0.1$ and $\beta = 4$, where $\alpha < 4\beta$.

In Fig. 6, the exact equilibrium paths, obtained from the numerical solution of Eq. (7), are shown in green when stable and in red when unstable, while the asymptotically determined bifurcated paths are shown in black when stable and in gray when unstable. In Fig. 6a,c, the paths are represented in the 3D (u_1, Δ, μ) space, with $\Delta \equiv u_2$, while in Fig. 6b,d, a 2D representation is provided in the (Δ, μ) plane. Generally, the curves from asymptotic analyses closely match the numerical ones in a neighborhood of the bifurcation points, to step away far from these points. In particular, by referring to the case $\alpha > 4\beta$, it is observed that the bifurcation point precedes the limit point on the fundamental path, emanating from the origin of the space/plane, while in the case $\alpha < 4\beta$, the bifurcation point follows the limit point. In both cases, no post-bifurcations are observed, consistently with the asymptotic analyses results.

In Fig. 7, the results concerning the system with three masses are analyzed; numerical results correspond to the solution of Eq. (9). In this case, Fig. 7a,c depict projections of equilibrium paths in the 3D space (u_1, u_2, Δ), where $\Delta \equiv u_3$, while Fig. 7b,d are analogous to those in Fig. 6. Similarly to the preceding system, an excellent agreement between numerical and asymptotic results is observed here close to bifurcations. Notably, bifurcation points precede or succeed the limit point on the fundamental path depending on whether $\alpha \gtrless 4\beta$; it is noteworthy that in the (u_1, u_2, Δ) space, the fundamental path appears as a straight line passing through the origin. In Fig. 7a, pertaining to the case $\alpha > 4\beta$, it can be observed that the bifurcated path $\mathcal{P}_2$, emanating from the point nearest to the origin, exhibits a post-bifurcation, and remarkably, there is a close correspondence between the predicted point via asymptotic and numerical analyses. Additionally, path $\mathcal{P}_1$ does not manifest post-bifurcated paths, although the asymptotic analyses (Eq. (45)), predicted post-bifurcations. This is due to the fact that the asymptotic approximation is too poor to describe with sufficient accuracy the exact path. Nevertheless, it is observed that this latter path exhibits a *limit point* with respect to Δ, which, although in an erroneous way, is found as branch points on the approximated path. This result could be proven to be general, but the relevant discussion is omitted here. Paths in Fig. 7c,d are qualitatively analogous.

The results depicted in Fig. 8 complement the scenario analyzed in this study. In Fig. 8a,c, projections of equilibrium paths in the 3D space (u_1, u_2, Δ), where $\Delta \equiv u_4$, are presented, while Fig. 8b,d are planar projections. Once again, an excellent agreement between asymptotic and purely numerical analyses is observable close to the bifurcation points. Furthermore, from the two case studies, it is evident that the bifurcation points either precede or succeed the limit point. Particularly in Fig. 8a, it is apparent that path $\mathcal{P}_2$ exhibits two post-bifurcations, consistent with the findings of Fig. 5. However, the results of asymptotic analyses in this instance are only qualitatively accurate, not quantitatively, as the post-bifurcation occurs far from the bifurcation. Analogous considerations to those made for the three-mass system

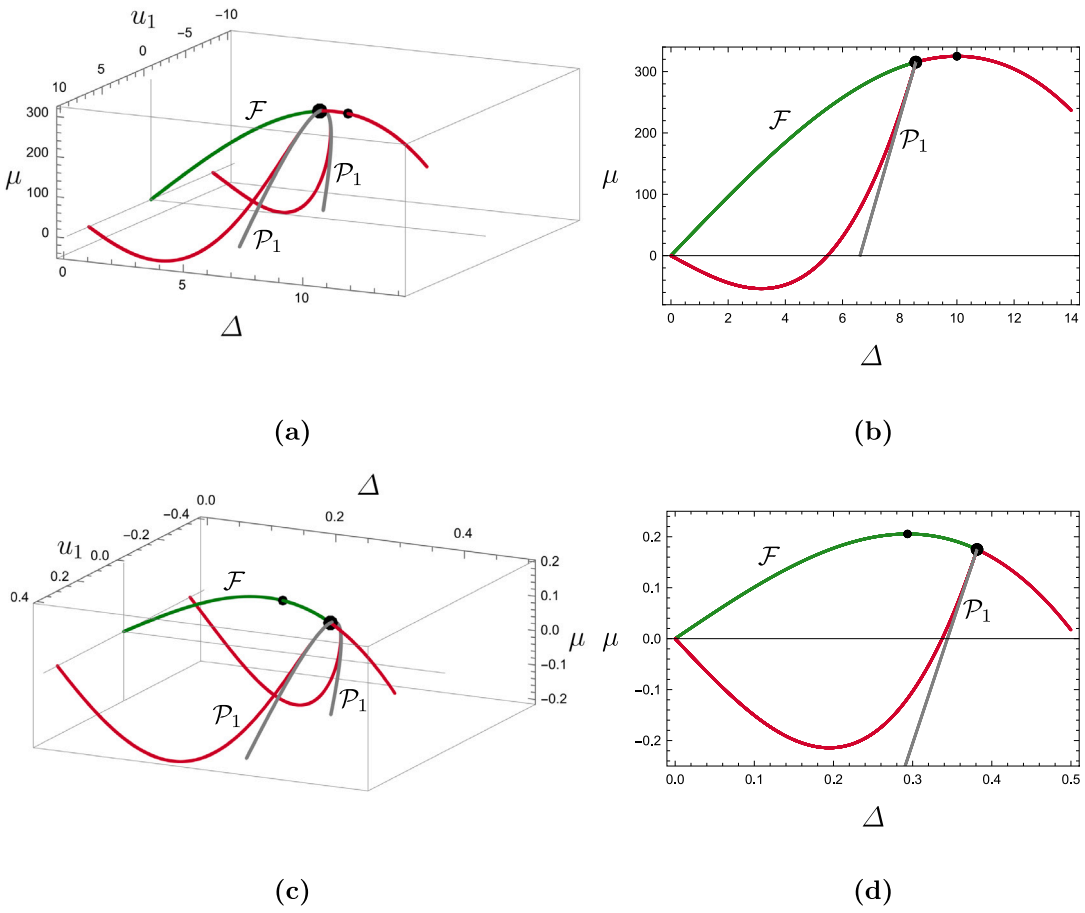

Fig. 6. Equilibrium paths of the two mass chain: (a), (b) $\alpha = 16$ and $\beta = 0.1$ ($\alpha > 4\beta$); (c), (d) $\alpha = 0.1$ and $\beta = 4$ ($\alpha < 4\beta$). Asymptotic solutions are shown in black when stable and gray when unstable; numerical solutions are shown in green when stable and red when unstable. (For interpretation of the references to color in this figure legend, the reader is referred to the web version of this article.)

hold for the other predicted post-bifurcation points on $\mathcal{P}_{1,3}$, as discussed in Fig. 4.

7. Discussion, conclusions and future work

The critical and postcritical behavior of Fermi–Pasta–Ulam (FPU) chains has been studied. The chains are made of $n = 2, 3, 4$ masses, linked by nonlinear springs with softening cubic constitutive law, connecting adjacent masses (modeling first-order interactions) as well as alternate masses (modeling second-order interactions). The chain in fixed at the left end and subject to a prescribed displacement at the right end (equal to the total elongation of the chain), taken as bifurcation parameter; it has, therefore, $n - 1$ degrees of freedom. A fundamental path is found, along which the displacements of the mass increase proportionally to the bifurcation parameter, while the reactive force at the right end exhibits a limit point. Primary bifurcation points and related bifurcated paths branching from the fundamental path have been determined. A post bifurcation analysis of the primary bifurcated paths has been carried out, aimed to detect possible post-bifurcations. The stability of all the branches found has been ascertained by applying the Lagrange–Dirichlet theorem. The whole analysis has been performed analytically, by using asymptotic methods, and results validated by purely numerical investigations. The following main results have been drawn.

1. The mechanical behavior of the FPU chains is governed by two nondimensional parameters, α, β, which measure the second-to-first-order elastic constant ratio, for the linear and nonlinear parts of the constitutive law, respectively.
2. There exists a degenerate condition, i.e., $\alpha = 4\beta$, that identifies a degenerate condition in which all the primary bifurcations coalesce at the limit point. If $\alpha < 4\beta$ the bifurcations occur at the left of the limit point, if $\alpha > 4\beta$ on the right. Moreover, the critical modes appear as 'naturally' ordered (i.e., for decreasing wavelength) when $\alpha < 4\beta$ and in reverse order when $\alpha < 4\beta$. Only the non-degenerate case $\alpha - 4\beta = O(1)$, in which the bifurcations points are well-separated, has been studied in this paper.
3. The FPU chains exhibit a bifurcation scenario whose complexity increases with the number of masses n. The primary bifurcated paths are $n - 1$ in number. The buckling modes are sampled sinusoidal functions, so that they are symmetric or antisymmetric.

   (a) When $n = 2$, only one bifurcated path exists, generated by a sub-critical pitchfork bifurcation. It is unstable, irrespective of $\alpha \gtrless 4\beta$, and does not post-bifurcate.
   (b) When $n = 3$, there exist two primary bifurcated paths, one associated with a symmetric (S), the other with an antisymmetric (A) buckling mode. The S-path is generated by a pitchfork bifurcation, which is super-critical when $\alpha > 4\beta$ and sub-critical when $\alpha < 4\beta$. The response along the S-path changes from symmetric to non-symmetric,

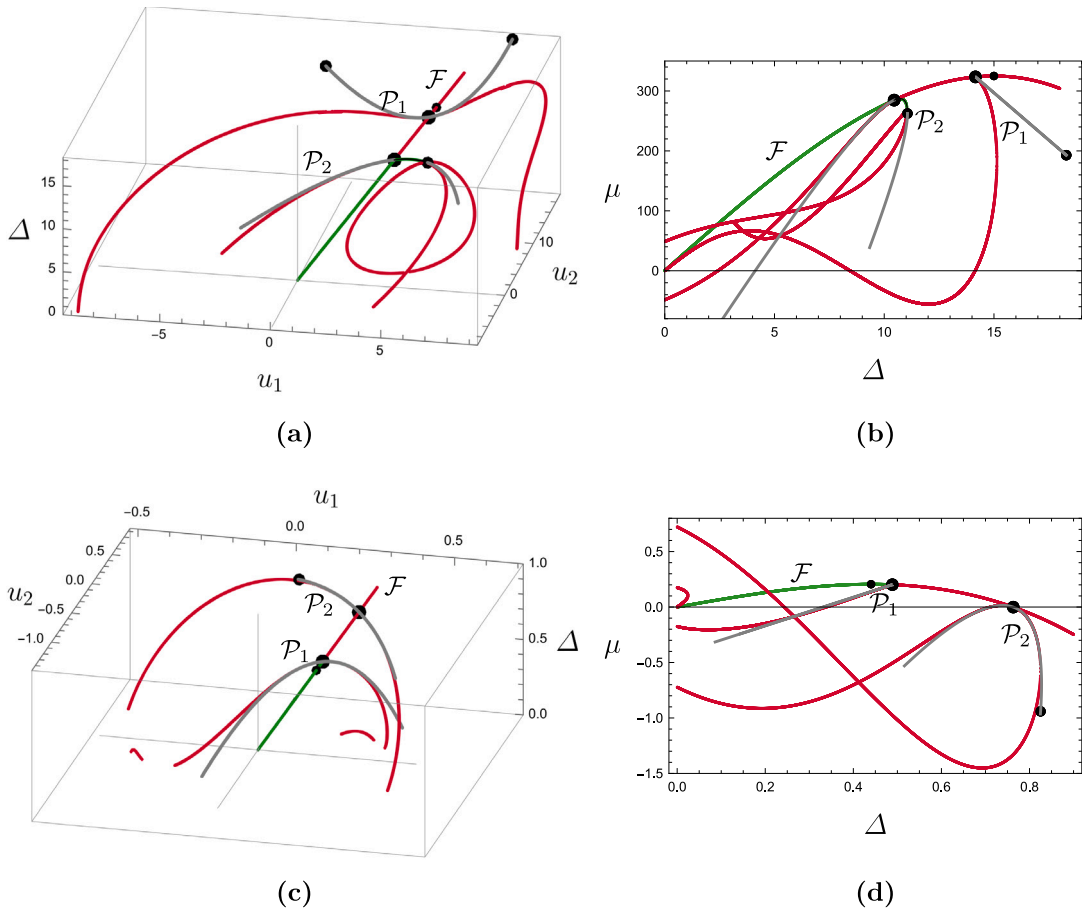

Fig. 7. Equilibrium paths of the three mass chain: (a), (b) $\alpha = 16$ and $\beta = 0.1$ ($\alpha > 4\beta$); (c), (d) $\alpha = 0.1$ and $\beta = 4$ ($\alpha < 4\beta$). Asymptotic solutions are shown in black when stable and gray when unstable; numerical solutions are shown in green when stable and red when unstable. (For interpretation of the references to color in this figure legend, the reader is referred to the web version of this article.)

since nonlinearities triggers antisymmetric corrections, whose sign depends on $\alpha \gtrless 4\beta$. The *A*-path, instead, is generated by a transcritical bifurcation; its slope at the bifurcation point has a sign which depends on $\beta \lessgtr \frac{1}{2}$ and zeroes in the special case $\beta = \frac{1}{2}$, for which the bifurcation becomes a sub-critical pitchfork. The response along the *A*-path remains antisymmetric, to within the order of the perturbation expansion carried out. Concerning secondary bifurcations, the *S*-path can post-bifurcate or not depending on the values of the parameters α and β, while the *A*-path does, at a value of the incremental elongation (with respect that on the fundamental path) which is positive or negative according to $\alpha \gtrless 4\beta$. Concerning stability, the *S*-path is always unstable; the *A*-path, instead, follows a more complex rule: (i) it is unstable if $\alpha < 4\beta$ (i.e., when it is the highest mode), (ii) it is stable when $\alpha > 4\beta$ (i.e., when it is the lowest mode), but only if $\beta < \frac{1}{2}$ and, however, only before the occurrence of the post-bifurcation, at which it loses stability; (iii) it is unstable if $\alpha < 4\beta$ and $\beta > \frac{1}{2}$.

(c) When $n = 4$, there exist three bifurcated paths, whose buckling modes, naturally ordered, are: one symmetric of large wavelength (*LS*), one antisymmetric (*A*), one symmetric of small wavelength (*SS*). Both the *S*-paths are corrected by antisymmetric components triggered by nonlinearities, while the *A*-path is unaffected by corrections, thus remaining antisymmetric (as in the $n = 3$ case). The *S*-paths possibly post-bifurcate in a even number of points (i.e., 0, 2, 4) according to combinations of the parameters, which fall in regions of the (α, β)-plane, which have been determined in a map, built-up analytically. Post-bifurcations occur in pairs relevant to equal and opposite values of the incremental elongation. The *A*-path also post-bifurcates in an even number (i.e., 0, 2, 4) of generally not symmetrically disposed points, according to a similar map. Stability of the bifurcated paths could be ascertained by numerically evaluating the Hessian of the total potential energy, but this has been omitted here for the sake of brevity.

4. When the loading process is displacement-controlled, the chain can only lose stability via a branch point; when it is force-controlled, also via a limit point. The topic has been discussed with reference to the $n = 2$ chain. It is stressed, however, that the asymptotic analysis demands that the fundamental path is expressed by a single-valued function, which suggests using the displacement (and not the force) as the bifurcation parameter.

As further developments of the research, nowadays in progress, two aspects of the problem should be investigated. The first concerns the analysis of the degenerate case $\alpha = 4\beta$, in which it is expected that all primary and secondary paths bifurcate from the limit point, via a mechanism which is well exemplified by the Augusti Model [25]. Moreover, the analysis of the nearly-degenerate case $\alpha \simeq 4\beta$ should explain *how* such bifurcated paths split to generate the scenario illustrated here for the non-degenerate case. The second aspect to be analyzed concerns the effect of imperfections in both non-degenerate

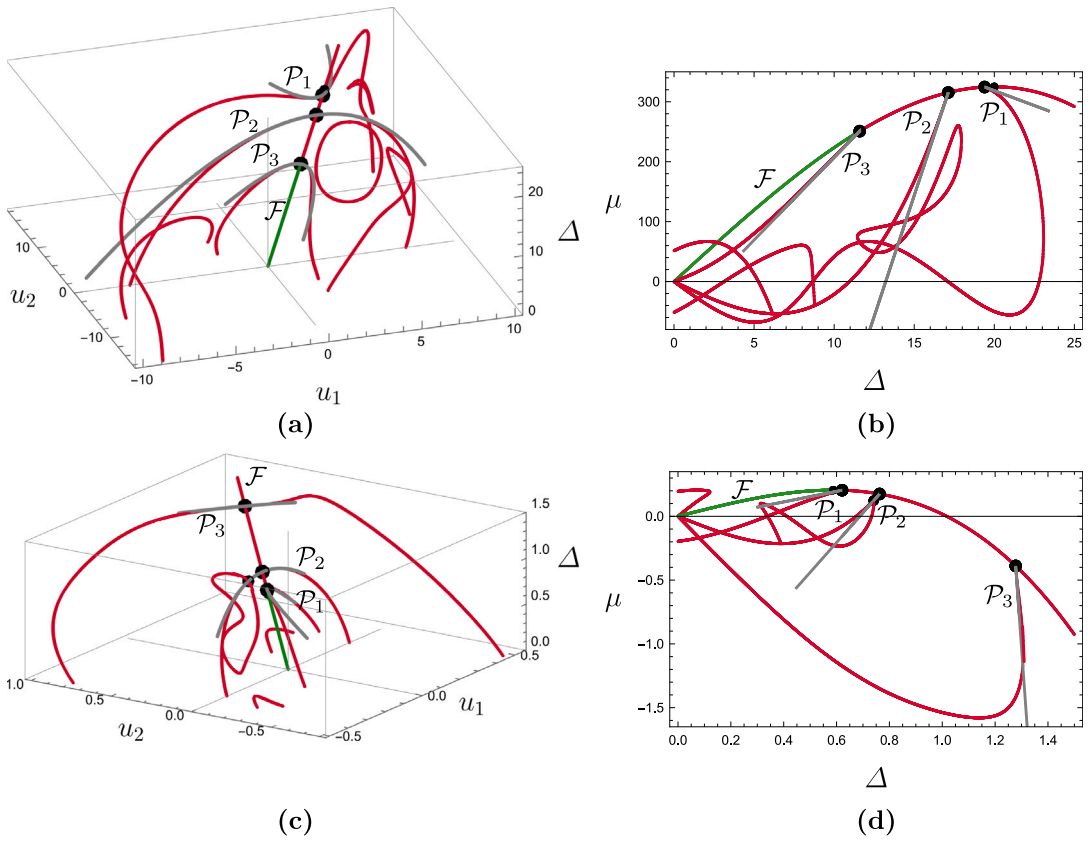

Fig. 8. Equilibrium paths of the four mass chain: (a), (b) $\alpha = 16$ and $\beta = 0.1$ ($\alpha > 4\beta$); (c), (d) $\alpha = 0.1$ and $\beta = 4$ ($\alpha < 4\beta$). Asymptotic solutions are shown in black when stable and gray when unstable; numerical solutions are shown in green when stable and red when unstable. (For interpretation of the references to color in this figure legend, the reader is referred to the web version of this article.)

and nearly- or perfectly-degenerate cases. It is expected that when the modes are well-separated, imperfections mainly affect the single modes via modal projections. In contrast, when the modes interact as nearly-simultaneous, the imperfect paths could develop in the whole configuration space, before being attracted by a specific path, an interesting question deserving attention.

CRediT authorship contribution statement

Angelo Luongo: Writing – review & editing, Writing – original draft, Methodology, Investigation, Conceptualization. **Manuel Ferretti:** Writing – review & editing, Writing – original draft, Methodology, Investigation, Conceptualization. **Noël Challamel:** Writing – review & editing, Writing – original draft, Methodology, Investigation, Conceptualization.

Declaration of competing interest

The authors declare that they have no known competing financial interests or personal relationships that could have appeared to influence the work reported in this paper.

Appendix A. Equilibrium equations and hessian matrices

The equilibrium equations for the $n = 3, 4$ chains are derived. Moreover, the Hessian matrix of the TPE for $n = 2, 3, 4$ are computed.

Equilibrium equations. The nondimensional TPE of the three-mass chain (Fig. 1b), by using the quantities defined in Eq. (5), is:

$$\begin{aligned} W = {} & \frac{1}{2}(1+2\alpha)u_1^2 - \frac{1}{12}(1+8\beta)u_1^4 + \frac{1}{2}(1+2\alpha)(u_3-u_2)^2 \\ & - \frac{1}{12}(1+8\beta)(u_3-u_2)^4 + \frac{1}{2}(u_2-u_1)^2 - \frac{1}{12}(u_2-u_1)^4 \\ & + \frac{1}{2}\alpha u_2^2 - \frac{1}{12}\beta u_2^4 + \frac{1}{2}\alpha(u_3-u_1)^2 - \frac{1}{12}\beta(u_3-u_1)^4 - \frac{2}{3}\mu u_3. \end{aligned} \tag{A.1}$$

From it, the equilibrium Eq. (9) follow, in which:

$$\begin{pmatrix} f_1 \\ f_2 \\ f_3 \end{pmatrix} := \frac{1}{3}\begin{pmatrix} \beta(u_3-u_1)^3 + (u_2-u_1)^3 - (1+8\beta)u_1^3 \\ (1+8\beta)(u_3-u_2)^3 + (u_1-u_2)^3 - \beta u_2^3 \\ \beta(u_1-u_3)^3 + (1+8\beta)(u_2-u_3)^3 \end{pmatrix}. \tag{A.2}$$

Analogously, the TPE of the four-mass chain (Fig. 1c) is:

$$\begin{aligned} W = {} & \frac{1}{2}(1+2\alpha)u_1^2 - \frac{1}{12}(1+8\beta)u_1^4 + \frac{1}{2}(1+2\alpha)(u_4-u_3)^2 \\ & - \frac{1}{12}(1+8\beta)(u_4-u_3)^4 + \frac{1}{2}(u_2-u_1)^2 - \frac{1}{12}(u_2-u_1)^4 \\ & + \frac{1}{2}(u_3-u_2)^2 - \frac{1}{12}(u_3-u_2)^4 + \frac{1}{2}\alpha u_2^2 - \frac{1}{12}\beta u_2^4 \\ & + \frac{1}{2}\alpha(u_3-u_1)^2 - \frac{1}{12}\beta(u_3-u_1)^4 + \frac{1}{2}\alpha(u_4-u_2)^2 \\ & - \frac{1}{12}\beta(u_4-u_2)^4 - \frac{2}{3}\mu u_4, \end{aligned} \tag{A.3}$$

which leads to the equilibrium Eq. (10), in which:

$$\begin{pmatrix} f_1 \\ f_2 \\ f_3 \\ f_4 \end{pmatrix} := \frac{1}{3}\begin{pmatrix} \beta(u_3-u_1)^3 + (u_2-u_1)^3 - (1+8\beta)u_1^3 \\ \beta(u_4-u_2)^3 + (u_1-u_2)^3 + (u_3-u_2)^3 - \beta u_2^3 \\ \beta(u_1-u_3)^3 + (1+8\beta)(u_4-u_3)^3 + (u_2-u_3)^3 \\ \beta(u_2-u_4)^3 + (1+8\beta)(u_3-u_4)^3 \end{pmatrix}. \tag{A.4}$$

Hessian matrices of the TPE. The Hessian matrices of the TPE, in the context of displacement-driven loading, are derived from the second

$$\mathbf{K}(\mathbf{u};\Delta)=\begin{bmatrix} 3\alpha+2-(1+8\beta)u_1^2 & (u_2-u_1)^2-1 & \beta(u_3-u_1)^2-\alpha \\ -\beta(u_3-u_1)^2-(u_2-u_1)^2 & 2(1+\alpha)-\beta(\Delta-u_2)^2-\beta u_2^2 & (u_3-u_2)^2-1 \\ & -(u_2-u_1)^2-(u_3-u_2)^2 & \\ & & 3\alpha+2-(1+8\beta)(\Delta-u_3)^2 \\ \text{SYM} & & -\beta(u_3-u_1)^2-(u_3-u_2)^2 \end{bmatrix}. \tag{A.7}$$

Box II.

variation of Eqs. (6), (A.1), (A.3). The following results are obtained. For $n=2$:

$$\mathbf{K}(\mathbf{u};\Delta)=\left[2+4\alpha-(1+8\beta)\left(\Delta^2-2\Delta u_1+2u_1^2\right)\right], \tag{A.5}$$

for $n=3$:

$$\mathbf{K}(\mathbf{u};\Delta)=\begin{bmatrix} 3\alpha+2-\beta(\Delta-u_1)^2 & (u_2-u_1)^2-1 \\ -(1+8\beta)u_1^2-(u_2-u_1)^2 & \\ & 3\alpha+2-(u_2-u_1)^2 \\ \text{SYM} & -(1+8\beta)(\Delta-u_2)^2-\beta u_2^2 \end{bmatrix}, \tag{A.6}$$

for $n=4$, as given in Eq. (A.7) in Box II.

Appendix B. Nonlinear terms of Eq. (17)

The components of the vectors, $\ddot{\mathbf{f}}_c=(\ddot{f}_{ci})$, $\dddot{\mathbf{f}}_c=(\dddot{f}_{ci})$, $i=1,\dots,n-1$, appearing in the perturbation Eq. (17), are reported here. For the $n=3$ chain they are:

$$\begin{aligned}\ddot{f}_{c1} :=& \left(-\frac{2}{3}\dot{v}_{1c}\dot{v}_{2c}-2\beta\dot{v}_{1c}^2+\frac{1}{3}\dot{v}_{2c}^2\right)\Delta_c \\ &+\left(-\frac{8}{3}\beta\dot{v}_{1c}-\frac{4}{9}\dot{v}_{1c}+\frac{2\dot{v}_{2c}}{9}\right)\Delta_c\dot{\Delta}_c,\end{aligned} \tag{B.1}$$

$$\begin{aligned}\ddot{f}_{c2} :=& \left(\frac{2}{3}\dot{v}_{1c}\dot{v}_{2c}-\frac{1}{3}\dot{v}_{1c}^2+2\beta\dot{v}_{2c}^2\right)\Delta_c \\ &+\left(\frac{2\dot{v}_{1c}}{9}-\frac{8}{3}\beta\dot{v}_{2c}-\frac{4\dot{v}_{2c}}{9}\right)\Delta_c\dot{\Delta}_c,\end{aligned} \tag{B.2}$$

and:

$$\begin{aligned}\dddot{f}_{c1} :=& \dot{v}_{1c}^2\dot{v}_{2c}-\dot{v}_{1c}\dot{v}_{2c}^2-3\beta\dot{v}_{1c}^3-\frac{2}{3}\dot{v}_{1c}^3+\frac{1}{3}\dot{v}_{2c}^3 \\ &+\left(-\frac{2}{3}\dot{v}_{2c}\ddot{v}_{1c}-\frac{2}{3}\dot{v}_{1c}\ddot{v}_{2c}-4\beta\dot{v}_{1c}\ddot{v}_{1c}+\frac{2}{3}\dot{v}_{2c}\ddot{v}_{2c}\right)\Delta_c \\ &+\left(-\frac{2}{3}\dot{v}_{1c}\dot{v}_{2c}-2\beta\dot{v}_{1c}^2+\frac{1}{3}\dot{v}_{2c}^2\right)\dot{\Delta}_c \\ &+\left(-\frac{8}{3}\beta\ddot{v}_{1c}-\frac{4}{9}\ddot{v}_{1c}+\frac{2\ddot{v}_{2c}}{9}\right)\Delta_c\dot{\Delta}_c \\ &+\left(-\frac{4}{3}\beta\dot{v}_{1c}-\frac{2}{9}\dot{v}_{1c}+\frac{\dot{v}_{2c}}{9}\right)\dot{\Delta}_c^2 \\ &+\left(-\frac{8}{3}\beta\dot{v}_{1c}-\frac{4}{9}\dot{v}_{1c}+\frac{2\dot{v}_{2c}}{9}\right)\Delta_c\ddot{\Delta}_c,\end{aligned} \tag{B.3}$$

$$\begin{aligned}\dddot{f}_{c2} :=& -\dot{v}_{1c}^2\dot{v}_{2c}+\dot{v}_{1c}\dot{v}_{2c}^2+\frac{1}{3}\dot{v}_{1c}^3-3\beta\dot{v}_{2c}^3-\frac{2}{3}\dot{v}_{2c}^3 \\ &+\left(\frac{2}{3}\dot{v}_{2c}\ddot{v}_{1c}+\frac{2}{3}\dot{v}_{1c}\ddot{v}_{2c}-\frac{2}{3}\dot{v}_{1c}\ddot{v}_{1c}+4\beta\dot{v}_{2c}\ddot{v}_{2c}\right)\Delta_c \\ &+\left(\frac{2}{3}\dot{v}_{1c}\dot{v}_{2c}-\frac{1}{3}\dot{v}_{1c}^2+2\beta\dot{v}_{2c}^2\right)\dot{\Delta}_c \\ &+\left(\frac{2\ddot{v}_{1c}}{9}-\frac{8}{3}\beta\ddot{v}_{2c}-\frac{4\ddot{v}_{2c}}{9}\right)\Delta_c\dot{\Delta}_c \\ &+\left(\frac{\dot{v}_{1c}}{9}-\frac{4}{3}\beta\dot{v}_{2c}-\frac{2\dot{v}_{2c}}{9}\right)\dot{\Delta}_c^2 \\ &+\left(\frac{2\dot{v}_{1c}}{9}-\frac{8}{3}\beta\dot{v}_{2c}-\frac{4\dot{v}_{2c}}{9}\right)\Delta_c\ddot{\Delta}_c.\end{aligned} \tag{B.4}$$

For the $n=4$ chain:

$$\begin{aligned}\ddot{f}_{c1} :=& \left(-\frac{1}{2}\dot{v}_{1c}\dot{v}_{2c}-\beta\dot{v}_{1c}\dot{v}_{3c}-\frac{3}{2}\beta\dot{v}_{1c}^2+\frac{1}{4}\dot{v}_{2c}^2+\frac{1}{2}\beta\dot{v}_{3c}^2\right)\Delta_c \\ &+\left(-\frac{3}{2}\beta\dot{v}_{1c}-\frac{1}{4}\dot{v}_{1c}+\frac{\dot{v}_{2c}}{8}+\frac{1}{2}\beta\dot{v}_{3c}\right)\Delta_c\dot{\Delta}_c\end{aligned} \tag{B.5}$$

$$\begin{aligned}\ddot{f}_{c2} :=& \left(\frac{1}{2}\dot{v}_{1c}\dot{v}_{2c}-\frac{1}{4}\dot{v}_{1c}^2-\frac{1}{2}\dot{v}_{2c}\dot{v}_{3c}+\frac{1}{4}\dot{v}_{3c}^2\right)\Delta_c \\ &+\left(\frac{\dot{v}_{1c}}{8}-\beta\dot{v}_{2c}-\frac{\dot{v}_{2c}}{4}+\frac{\dot{v}_{3c}}{8}\right)\Delta_c\dot{\Delta}_c,\end{aligned} \tag{B.6}$$

$$\begin{aligned}\ddot{f}_{c3} :=& \left(\beta\dot{v}_{1c}\dot{v}_{3c}-\frac{1}{2}\beta\dot{v}_{1c}^2+\frac{1}{2}\dot{v}_{2c}\dot{v}_{3c}-\frac{1}{4}\dot{v}_{2c}^2+\frac{3}{2}\beta\dot{v}_{3c}^2\right)\Delta_c \\ &+\left(\frac{1}{2}\beta\dot{v}_{1c}+\frac{\dot{v}_{2c}}{8}-\frac{3}{2}\beta\dot{v}_{3c}-\frac{\dot{v}_{3c}}{4}\right)\Delta_c\dot{\Delta}_c,\end{aligned} \tag{B.7}$$

and:

$$\begin{aligned}\dddot{f}_{c1} :=& \dot{v}_{1c}^2\dot{v}_{2c}-\dot{v}_{1c}\dot{v}_{2c}^2+\beta\dot{v}_{1c}^2\dot{v}_{3c}-\beta\dot{v}_{1c}\dot{v}_{3c}^2-3\beta\dot{v}_{1c}^3-\frac{2}{3}\dot{v}_{1c}^3 \\ &+\frac{1}{3}\dot{v}_{2c}^3+\frac{1}{3}\beta\dot{v}_{3c}^3 \\ &+\left(-\frac{1}{2}\dot{v}_{2c}\ddot{v}_{1c}-\frac{1}{2}\dot{v}_{1c}\ddot{v}_{2c}-\beta\dot{v}_{3c}\ddot{v}_{1c}-\beta\dot{v}_{1c}\ddot{v}_{3c}-3\beta\dot{v}_{1c}\ddot{v}_{1c}\right. \\ &\left.+\frac{1}{2}\dot{v}_{2c}\ddot{v}_{2c}+\beta\dot{v}_{3c}\ddot{v}_{3c}\right)\Delta_c \\ &+\left(-\frac{1}{2}\dot{v}_{1c}\dot{v}_{2c}-\beta\dot{v}_{1c}\dot{v}_{3c}-\frac{3}{2}\beta\dot{v}_{1c}^2+\frac{1}{4}\dot{v}_{2c}^2+\frac{1}{2}\beta\dot{v}_{3c}^2\right)\dot{\Delta}_c \\ &+\left(-\frac{3}{2}\beta\ddot{v}_{1c}-\frac{1}{4}\ddot{v}_{1c}+\frac{\ddot{v}_{2c}}{8}+\frac{1}{2}\beta\ddot{v}_{3c}\right)\Delta_c\dot{\Delta}_c \\ &+\left(-\frac{3}{4}\beta\dot{v}_{1c}-\frac{1}{8}\dot{v}_{1c}+\frac{\dot{v}_{2c}}{16}+\frac{1}{4}\beta\dot{v}_{3c}\right)\dot{\Delta}_c^2 \\ &+\left(-\frac{3}{2}\beta\dot{v}_{1c}-\frac{1}{4}\dot{v}_{1c}+\frac{\dot{v}_{2c}}{8}+\frac{1}{2}\beta\dot{v}_{3c}\right)\Delta_c\ddot{\Delta}_c,\end{aligned} \tag{B.8}$$

$$\begin{aligned}\dddot{f}_{c2} :=& -\dot{v}_{1c}^2\dot{v}_{2c}+\dot{v}_{1c}\dot{v}_{2c}^2+\frac{1}{3}\dot{v}_{1c}^3-\dot{v}_{2c}\dot{v}_{3c}^2+\dot{v}_{2c}^2\dot{v}_{3c}-\frac{2}{3}\beta\dot{v}_{2c}^3-\frac{2}{3}\dot{v}_{2c}^3+\frac{1}{3}\dot{v}_{3c}^3 \\ &+\left(\frac{1}{2}\dot{v}_{2c}\ddot{v}_{1c}+\frac{1}{2}\dot{v}_{1c}\ddot{v}_{2c}-\frac{1}{2}\dot{v}_{1c}\ddot{v}_{1c}-\frac{1}{2}\dot{v}_{3c}\ddot{v}_{2c}-\frac{1}{2}\dot{v}_{2c}\ddot{v}_{3c}+\frac{1}{2}\dot{v}_{3c}\ddot{v}_{3c}\right)\Delta_c \\ &+\left(\frac{1}{2}\dot{v}_{1c}\dot{v}_{2c}-\frac{1}{4}\dot{v}_{1c}^2-\frac{1}{2}\dot{v}_{2c}\dot{v}_{3c}+\frac{1}{4}\dot{v}_{3c}^2\right)\dot{\Delta}_c \\ &+\left(\frac{\ddot{v}_{1c}}{8}-\beta\ddot{v}_{2c}-\frac{\ddot{v}_{2c}}{4}+\frac{\ddot{v}_{3c}}{8}\right)\Delta_c\dot{\Delta}_c \\ &+\left(\frac{\dot{v}_{1c}}{16}-\frac{1}{2}\beta\dot{v}_{2c}-\frac{\dot{v}_{2c}}{8}+\frac{\dot{v}_{3c}}{16}\right)\dot{\Delta}_c^2 \\ &+\left(\frac{\dot{v}_{1c}}{8}-\beta\dot{v}_{2c}-\frac{\dot{v}_{2c}}{4}+\frac{\dot{v}_{3c}}{8}\right)\Delta_c\ddot{\Delta}_c,\end{aligned} \tag{B.9}$$

$$\begin{aligned}\dddot{f}_{c3} :=& -\beta\dot{v}_{1c}^2\dot{v}_{3c}+\beta\dot{v}_{1c}\dot{v}_{3c}^2+\frac{1}{3}\beta\dot{v}_{1c}^3+\dot{v}_{2c}\dot{v}_{3c}^2-\dot{v}_{2c}^2\dot{v}_{3c} \\ &+\frac{1}{3}\dot{v}_{2c}^3-3\beta\dot{v}_{3c}^3-\frac{2}{3}\dot{v}_{3c}^3 \\ &+\left(\beta\dot{v}_{3c}\ddot{v}_{1c}+\beta\dot{v}_{1c}\ddot{v}_{3c}-\beta\dot{v}_{1c}\ddot{v}_{1c}+\frac{1}{2}\dot{v}_{3c}\ddot{v}_{2c}+\frac{1}{2}\dot{v}_{2c}\ddot{v}_{3c}\right. \\ &\left.-\frac{1}{2}\dot{v}_{2c}\ddot{v}_{2c}+3\beta\dot{v}_{3c}\ddot{v}_{3c}\right)\Delta_c \\ &+\left(\frac{1}{4}\beta\dot{v}_{1c}+\frac{\dot{v}_{2c}}{16}-\frac{3}{4}\beta\dot{v}_{3c}-\frac{\dot{v}_{3c}}{8}\right)\dot{\Delta}_c^2 \\ &+\left(\frac{1}{2}\beta\ddot{v}_{1c}+\frac{\ddot{v}_{2c}}{8}-\frac{3}{2}\beta\ddot{v}_{3c}-\frac{\ddot{v}_{3c}}{4}\right)\Delta_c\dot{\Delta}_c \\ &+\left(\beta\dot{v}_{1c}\dot{v}_{3c}-\frac{1}{2}\beta\dot{v}_{1c}^2+\frac{1}{2}\dot{v}_{2c}\dot{v}_{3c}-\frac{1}{4}\dot{v}_{2c}^2+\frac{3}{2}\beta\dot{v}_{3c}^2\right)\dot{\Delta}_c \\ &+\left(\frac{1}{2}\beta\dot{v}_{1c}+\frac{\dot{v}_{2c}}{8}-\frac{3}{2}\beta\dot{v}_{3c}-\frac{\dot{v}_{3c}}{4}\right)\Delta_c\ddot{\Delta}_c.\end{aligned} \tag{B.10}$$

Appendix C. Discussion of the quartic Eq. (57)

The number of real roots ϵ_{b2} of the quartic characteristic equation, obtained from the factorization of Eq. (57) (and relevant to the path $\mathcal{P}_2$ of the four-mass chain), is discussed based on the results reported in [26]. As is well known, by introducing the change of variable $\epsilon_{b2} = x - \frac{c_1}{4c_0}$ (see, e.g., [27]), the complete equation can be reduced to

$$x^4 + Px^2 + Qx + R = 0, \tag{C.1}$$

where P, Q, and R are real functions of the coefficients $c_k = c_k(\alpha, \beta)$. The reduced quartic Eq. (C.1), with $Q \neq 0$, and discriminant

$$\begin{aligned} D :=& \frac{4\left(P^2+12R\right)^3 - \left(2P^3 - 72PR + 27Q^2\right)^2}{27} \\ =& 16P^4R - 4P^3Q^2 - 128P^2R^2 + 144PQ^2R - 27Q^4 + 256R^3, \end{aligned} \tag{C.2}$$

admits [26]:

- four distinct real roots if $P < 0$, $4R - P^2 < 0$, and $D > 0$;
- no real roots if at least one of the conditions $P > 0$ or $4R - P^2 > 0$ holds, and $D > 0$;
- two distinct real and two complex conjugate roots if $D < 0$;
- at least one double real root if $D = 0$.

As highlighted in [26], the proof of these results is due to Lagrange [28].

The above conditions define the root map of ϵ_{b2}, as illustrated in Fig. 5.

Appendix D. Stability of the fundamental path in force-controlled loadings

If the loading process of the chain is driven by the force μ (and not by the displacement Δ), it is expected that stability of the fundamental path $\mathcal{F}$ is affected by the occurrence of the limit point L, in addition to the primary bifurcation points C_m. The topic is discussed, as an example, by referring to the simplest two-mass chain.

The TPE of the chain is expressed by Eq. (6), in which u_2 is a Lagrangian parameter, and μu_2 is an active work. The second variation of the TPE provides the Hessian matrix at a generic $\mathbf{u} = (u_1, u_2)$ point, i.e.:

$$\mathbf{K}(\mathbf{u};\mu) = \begin{bmatrix} 4\alpha + 2 & (8\beta+1)(u_1-u_2)^2 - 2\alpha - 1 \\ -(8\beta+1)\left(2u_1^2 - 2u_1u_2 + u_2^2\right) & \\ \text{SYM} & 3\alpha + 1 - \beta u_2^2 \\ & -(8\beta+1)(u_1-u_2)^2 \end{bmatrix}. \tag{D.1}$$

When the matrix is evaluated on the fundamental path $\hat{u}_1 = \frac{1}{2}\hat{u}_2$, it becomes:

$$\mathbf{K}(\hat{\mathbf{u}}(\mu);\mu) = \begin{bmatrix} 4\alpha + 2 - \frac{1}{2}(8\beta+1)\hat{u}_2^2 & \left(2\beta + \frac{1}{4}\right)\hat{u}_2^2 - 2\alpha - 1 \\ \text{SYM} & 3\alpha + 1 - \left(3\beta + \frac{1}{4}\right)\hat{u}_2^2 \end{bmatrix}, \tag{D.2}$$

in which $\hat{u}_2 = \hat{u}_2(\mu)$ is not free, but related to the assigned load μ by the last of the equilibrium condition in Eq. (7). However, such a dependence cannot be made explicit, since the function is not single-valued. Therefore, stability is studied as dependent on $\hat{u}_2$, and the relevant results attributed to the values of μ in equilibrium with $\hat{u}_2$.

The stability of the fundamental path is governed by the (real) eigenvalues $\lambda_{1,2}$ of $\mathbf{K}(\hat{\mathbf{u}}(\mu);\mu)$; however, since they assume a cumbersome form, the invariants of the matrix, $I_1 := \mathrm{tr}\left[\mathbf{K}(\hat{\mathbf{u}}(\mu);\mu)\right]$ and $I_2 := \det\left[\mathbf{K}(\hat{\mathbf{u}}(\mu);\mu)\right]$ are instead discussed, being $I_1 = \lambda_1 + \lambda_2$, $I_2 = \lambda_1\lambda_2$. The first invariant is linear in $\hat{u}_2^2$; it zeroes at:

$$\hat{u}_{2T} := 2\sqrt{\frac{7\alpha+3}{28\beta+3}}, \tag{D.3}$$

and it is positive on the left, negative on the right. The second invariant is parabolic in $\hat{u}_2^2$; it zeroes at:

$$\hat{u}_{2L} := 2\sqrt{\frac{1+4\alpha}{1+16\beta}}, \qquad \hat{u}_{2C} =: 2\sqrt{\frac{1+2\alpha}{1+8\beta}}, \tag{D.4}$$

and it is positive externally to the two roots, and negative internally. Here, $\hat{u}_{2L} \equiv \Delta_L$ (first of Eq. (13)) is the displacement of the end mass at the limit point, and $\hat{u}_{2C} \equiv \Delta_{c1}$ (Eq. (19)) is the displacement of the end mass at the (unique) bifurcation point of the displacement-controlled loading process. The corresponding values of the load are: μ_L, as given by the second of Eq. (13), and μ_C, as expressed by the first of Eq. (29). Hence, the present analysis provides the branching point C_1 already determined, together with the limit point L (which is instead absent in the displacement-controlled process). As a matter of fact, the stiffness matrix is one-dimensional when u_2 governs the loading process (Eq. (18)), while it is two-dimensional when μ governs it (Eq. (D.2)).

Based on the dependence of the invariants on $\hat{u}_2$, it follows:

- if $\alpha < 4\beta$, then $\hat{u}_{2L} < \hat{u}_{2T} < \hat{u}_{2C}$; this entails that $I_1 > 0$, $I_2 = 0$ at L (i.e., $\lambda_{1L} = 0$, $\lambda_{2L} > 0$), and $I_1 < 0$, $I_2 = 0$ at C_1 (i.e., $\lambda_{1C} < 0$, $\lambda_{2C} = 0$); it is concluded that the chain loses stability at the limit point, which is *not* regained at the successive branching point;
- if $\alpha > 4\beta$, then $\hat{u}_{2C} < \hat{u}_{2T} < \hat{u}_{2L}$; this entails that $I_1 > 0$, $I_2 = 0$ at C_1 (i.e., $\lambda_{1C} = 0$, $\lambda_{2C} > 0$), and $I_1 < 0$, $I_2 = 0$ at L (i.e., $\lambda_{1L} < 0$, $\lambda_{2L} = 0$); it is concluded that the chain loses stability at the branching point, which is *not* regained at the successive limit point.

Data availability

Data will be made available on request.

References

[1] I. Hegedüs, Branching of equilibrium paths in a deployable column, Int. J. Space Struct. 8 (1–2) (1993) 119–125.
[2] N. Friedman, M. Weiner, G. Farkas, I. Hegedüs, A. Ibrahimbegovic, On the snap-back behavior of a self-deploying antiprismatic column during packing, Eng. Struct. 50 (2013) 74–89.
[3] S. Guo, R. Gao, X. Tian, S. Liu, A quasi-zero-stiffness elastic metamaterial for energy absorption and shock attenuation, Eng. Struct. 280 (2023) 115687.
[4] M. Bodaghi, A.R. Damanpack, G.F. Hu, W.H. Liao, Large deformations of soft metamaterials fabricated by 3D printing, Mater. Des. 131 (2017) 81–91.
[5] M. Kucewicz, P. Baranowski, J. Małachowski, A. Popławski, P. Płatek, Modelling, and characterization of 3D printed cellular structures, Mater. Des. 142 (2018) 177–189.
[6] E. Dogan, A. Bhusal, B. Cecen, A.K. Miri, 3D printing metamaterials towards tissue engineering, Appl. Mater. Today 20 (2020) 100752.
[7] J.M.T. Thompson, G.W. Hunt, A General Theory of Elastic Stability, J. Wiley, 1973.
[8] Z.P. Bažant, L. Cedolin, Stability of Structures: Elastic, Inelastic, Fracture, and Damage Theories, Dover Publications, 2003.
[9] A.M.A. Van der Heijden, W. T. Koiter's Elastic Stability of Solids and Structures, Cambridge University Press, 2008.
[10] A. Luongo, M. Ferretti, S. Di Nino, Stability and Bifurcation of Structures: Statical and Dynamical Systems, Springer Nature, 2023.
[11] E. Fermi, P. Pasta, S. Ulam, M. Tsingou, Studies of the Nonlinear Problems, Technical Report, Los Alamos National Laboratory (LANL), Los Alamos, NM (United States), 1955.
[12] T. Dauxois, M. Peyrard, S. Ruffo, The Fermi–Pasta–Ulam 'numerical experiment': history and pedagogical perspectives, Eur. J. Phys. 26 (5) (2005) S3.
[13] T. Dauxois, M. Peyrard, Physics of Solitons, Cambridge University Press, 2006.
[14] A. Vainchtein, Solitary waves in FPU-type lattices, Phys. D: Nonlinear Phenom. 434 (2022) 133252.
[15] N. Triantafyllidis, S. Bardenhagen, On higher order gradient continuum theories in 1-D nonlinear elasticity. Derivation from and comparison to the corresponding discrete models, J. Elasticity 33 (1993) 259–293.
[16] L. Truskinovsky, A. Vainchtein, Quasicontinuum modelling of short-wave instabilities in crystal lattices, Phil. Mag. 85 (33–35) (2005) 4055–4065.
[17] C. Combescure, Selecting generalized continuum theories for nonlinear periodic solids based on the instabilities of the underlying microstructure, J. Elasticity 154 (1) (2023) 421–441.

[18] C. Findeisen, S. Forest, J. Hohe, P. Gumbsch, Discrete and continuum modelling of size effects in architectured unstable metamaterials, Contin. Mech. Thermodyn. 32 (2020) 1629–1645.
[19] N. Challamel, M. Ferretti, A. Luongo, Multi-degenerate hill-top bifurcation of Fermi–Pasta–Ulam softening chains: Exact and asymptotic solutions, Int. J. Non-Linear Mech. 156 (2023) 104509.
[20] M. Tanaka, K. Ikeda, F. Fujii, Versatile benchmark model reproducing snap-through, asymmetric, symmetric unstable/stable, and multiple bifurcation including hill-top branching in structural instability, Comput. Methods Appl. Mech. Engrg. 403 (2023) 115719.
[21] B. Hérisson, N. Challamel, V. Picandet, A. Perrot, Nonlocal continuum analysis of a nonlinear uniaxial elastic lattice system under non-uniform axial load, Phys. E: Low-Dimens. Syst. Nanostructures 83 (2016) 378–388.
[22] N. Challamel, C. Combescure, V. Picandet, M. Ferretti, A. Luongo, Exact bifurcation analysis of the static response of a Fermi–Pasta–Ulam softening chain with short and long-range interactions, Contin. Mech. Thermodyn. 37 (2) (2025) 1–30.
[23] M. Pignataro, N. Rizzi, A. Luongo, Stability, Bifurcation and Postcritical Behaviour of Elastic Structures, vol. 39, Elsevier, 2013.
[24] Wolfram Research, Inc., Mathematica, Version 13.1, Champaign, IL.
[25] G. Augusti, Stabilità di strutture elastiche elementari in presenza di grandi spostamenti, Atti Accad. Sci. Fis. Mat. Napoli 4 (5) (1967) Reprinted from the Series 3rd.
[26] L.E. Dickson, Elementary Theory of Equations, J. Wiley & Sons, 1914.
[27] A.D. Polyanin, A.V. Manzhirov, Handbook of Mathematics for Engineers and Scientists, Chapman and Hall/CRC, 2006.
[28] J.L. Lagrange, Traité de la résolution des équations numériques de tous les degrés, Bachelier, 1826.